Syst. Biol. 65(5):824–842, 2016

DOI:10.1093/sysbio/syw055
Advance Access publication June 10, 2016

Spatiotemporal Diversification of the True Frogs (Genus *Rana*): A Historical Framework for a Widely Studied Group of Model Organisms

ZHI-YONG YUAN[1,2], WEI-WEI ZHOU[1], XIN CHEN[3], NIKOLAY A. POYARKOV, JR.[4], HONG-MAN CHEN[1], NIAN-HONG JANG-LIAW[5], WEN-HAO CHOU[6], NICHOLAS J. MATZKE[7], KOJI IIZUKA[8], MI-SOOK MIN[9], SERGIUS L. KUZMIN[10], YA-PING ZHANG[1,*], DAVID C. CANNATELLA[11,*], DAVID M. HILLIS[11,*], AND JING CHE[1,*]

[1]*State Key Laboratory of Genetic Resources and Evolution, and Yunnan Laboratory of Molecular Biology of Domestic Animals, Kunming Institute of Zoology, Chinese Academy of Sciences, Kunming 650223, Yunnan;* [2]*Kunming College of Life Science, University of Chinese Academy of Sciences, Kunming 650204, Yunnan;* [3]*Department of Biological Sciences, Dartmouth College, Hanover, HN 03755, USA;* [4]*Department of Vertebrate Zoology, Biological Faculty, Lomonosov Moscow State University, Leninskiye Gory, GSP-1, Moscow 119991, Russia;* [5]*Animal Department, Taipei Zoo, 30 Xinguang Road, Sec. 2, Taipei 11656, Taiwan;* [6]*Department of Zoology, National Museum of Natural Science, 1st Kuang-Chien Road, Taichung 40453, Taiwan;* [7]*Division of Ecology, Evolution, and Genetics, Research School of Biology, The Australian National University, ACT 2601, Australia;* [8]*Kanda-Hitotsubashi JH School, 2-16-14 Hitotsubashi, Chiyoda-ku, Tokyo 101-0003, Japan;* [9]*Conservation Genome Resource Bank for Korean Wildlife (CGRB), Research Institute for Veterinary Science, College of Veterinary Medicine, Seoul National University, 151-742 Seoul, South Korea;* [10]*Institute of Ecology and Evolution, Russian Academy of Sciences, Moscow 119234, Russia; and* [11]*Department of Integrative Biology, University of Texas at Austin, Austin, TX 78712, USA*

**Correspondence to be sent to: Kunming Institute of Zoology, Chinese Academy of Sciences, Kunming 650223, Yunnan or Department of Integrative Biology, University of Texas at Austin, Austin, TX 78712, USA*
E-mail: chej@mail.kiz.ac.cn, dhillis@austin.utexas.edu, catfish@utexas.edu, zhangyp@mail.kiz.ac.cn

The first three authors share equal first authorship.

Received 19 September 2015; reviews returned 11 December 2015; accepted 31 May 2015
Associate Editor: Richard Glor

Abstract.—True frogs of the genus *Rana* are widely used as model organisms in studies of development, genetics, physiology, ecology, behavior, and evolution. Comparative studies among the more than 100 species of *Rana* rely on an understanding of the evolutionary history and patterns of diversification of the group. We estimate a well-resolved, time-calibrated phylogeny from sequences of six nuclear and three mitochondrial loci sampled from most species of *Rana*, and use that phylogeny to clarify the group's diversification and global biogeography. Our analyses consistently support an "Out of Asia" pattern with two independent dispersals of *Rana* from East Asia to North America via Beringian land bridges. The more species-rich lineage of New World *Rana* appears to have experienced a rapid radiation following its colonization of the New World, especially with its expansion into montane and tropical areas of Mexico, Central America, and South America. In contrast, Old World *Rana* exhibit different trajectories of diversification; diversification in the Old World began very slowly and later underwent a distinct increase in speciation rate around 29–18 Ma. Net diversification is associated with environmental changes and especially intensive tectonic movements along the Asian margin from the Oligocene to early Miocene. Our phylogeny further suggests that previous classifications were misled by morphological homoplasy and plesiomorphic color patterns, as well as a reliance primarily on mitochondrial genes. We provide a phylogenetic taxonomy based on analyses of multiple nuclear and mitochondrial gene loci. [Amphibians; biogeography; diversification rate; Holarctic; transcontinental dispersal.]

Biodiversity is distributed heterogeneously across Earth. Consequently, the determinants of spatial patterns of diversity are of paramount interest for biologists (Gaston 2000; Ricklefs 2004). Broadly distributed, species-rich clades provide an opportunity to explore the evolutionary processes that drive diversity across large spatiotemporal scales (e.g., Derryberry et al. 2011; McGuire et al. 2014). Methods combining the dynamics of diversification (e.g., speciation, extinction) with biogeographic history allow biologists to test hypotheses of diversification within and between regions (Ricklefs 2004; Wiens and Donoghue 2004; Mittelbach et al. 2007).

If speciation and extinction rates (ignoring dispersal for the moment) are roughly constant across geographic areas, then species diversity is influenced by time-dependent processes (McPeek and Brown 2007). However, changes in speciation rate (e.g., by adaptive radiations) or extinction rate (e.g., by climate effects) can quickly disrupt the correlation between clade age and species diversity. In many radiations, a pattern of early, rapid cladogenesis followed by a slowdown in diversification rate is thought to be related to ecological constraints (Schluter 2001; Rabosky 2009). Further, increases in cladogenesis are often associated with broad-scale environmental changes or geological processes (e.g., orogenesis).

Diverse clades that are distributed across several major continental areas provide excellent opportunities to compare patterns of distribution and diversification in different regions (Qian and Ricklefs 2000; McGuire et al. 2014). In this article we investigate the spatial and temporal patterns of regional and continental-scale biodiversity in a widely studied clade that is broadly distributed across Eurasia and the Americas, the true frogs (genus *Rana*, sensu AmphibiaWeb 2015).

True frogs are extensively used as model organisms in studies of development, genetics, physiology, behavior, ecology, and evolution (see Duellman and Trueb 1986). The first successful laboratory cloning experiment of an animal (transfer of a nucleus into an enucleated egg, resulting in a normal organism) was conducted

in *Rana pipiens* (Briggs and King 1952), and various species of *Rana* continue to be used widely in studies of physiology and genetics. Many species of *Rana* are also commonly studied in the field as well as the laboratory. One of the most extensive monographs on the ecology and life history of an amphibian was based on *Rana temporaria* (Savage 1962), and studies of *Rana* ecology, behavior, conservation, and evolution have accelerated in recent years (reviewed by Hillis and Wilcox 2005).

More than 100 described species of *Rana* (AmphibiaWeb 2015) range across Europe (12 species) and Asia (32 species), and from North America to the northern half of South America (57, plus several recognized but not yet described species; Hillis and Wilcox 2005). Species occur in a wide variety of habitats including tundra, temperate coniferous and deciduous forests, grasslands, deserts, brackish-water marshes, freshwater streams and lakes, montane cascades, semitropical cloud forests, and tropical rainforests (Hillis and Wilcox 2005). Many species are of conservation concern, and several species are recently extinct or threatened with extinction. Despite the diversity of the genus and its importance in many biological investigations, no comprehensive analysis of the spatial patterns and drivers of diversity for *Rana* has been published.

The Eurasian species are morphologically conservative. They possess prominent dorsolateral folds, a dark temporal mask, and a body that is countershaded in various shades of brown, leading to the common English name "brown frogs" (Boulenger 1920; Liu and Hu 1961). This color pattern occurs in many species in Europe, Asia, and North America, although several New World species groups show far greater morphological differentiation. This greater morphological diversity correlates with their varied ecologies, physiologies, behaviors, and morphological structures associated with mating calls and habitat (Hillis and Wilcox 2005). These differences in patterns of species diversity and biological divergence make *Rana* an excellent group for studying the processes of biodiversity generation.

Most previous studies of *Rana* have been restricted to particular geographic regions, or have used very limited sampling of global taxa, or have been limited to analyses of mtDNA sequences. For example, mtDNA analyses (sometimes with small amounts of nuclear DNA (nuDNA)) of *Rana* have included species in Europe (e.g., Veith et al. 2003), the New World (e.g., Hillis and Wilcox 2005), the mainland of East Asia (e.g., Che et al. 2007a), and the Asian islands (e.g., Tanaka-Ueno et al. 1998; Matsui 2011). We expand on these studies by analyzing six nuclear and three mitochondrial genes for a large majority of the extant species (90 species; Supplementary Table S1, available on Dryad at http://dx.doi.org/10.5061/dryad.ck1m7) across the entire distribution in Eurasia and the Americas, and by estimating divergence times and patterns of net diversification.

The family Ranidae began to diversify about 57 Ma (Bossuyt et al. 2006; Wiens et al. 2009), long after the breakup of Pangaea (>120 Ma, Sanmartín et al. 2001). Therefore, the global distribution of the family must have resulted from intercontinental dispersal. Based on limited sampling of *Rana*, Bossuyt et al. (2006) suggested that the ancestor(s) of the American *Rana* reached the New World in one or two waves from Eurasia, without specifying the route of dispersal. Macey et al. (2006) suggested two alternative hypotheses: two dispersals from Asia to America via Beringia, or one dispersal from Asia to America with a second back-dispersal to Asia. We asked the following questions:

(1) When did the intercontinental dispersal of *Rana* occur between Eurasia and the Americas? Were these dispersals via trans-Atlantic land bridges (Case 1978) or by trans-Beringian (Pacific) land bridges (Macey et al. 2006)? Was there only one dispersal from Eurasia to the Americas, with a dispersal back to Eurasia, or were there two distinct dispersal events into the New World? When did major dispersal events within Eurasia and the Americas occur (e.g., into Europe, and into the Neotropics)?

(2) To what extent was dispersal into new areas accompanied by increased diversification rates? Were speciation rates highest when a lineage entered new regions, or were they relatively constant?

(3) How did geologic events and environmental changes influence the diversification of *Rana* in the Old World (especially the diversity in East Asia) and the New World?

Materials and Methods

Taxon Sampling

Complete sampling of all species in *Rana* was a challenge due to the large number of species, their intercontinental distribution, and rarity or recent extinction of some species. Our analyses included 82 of the currently recognized species of *Rana* as well as eight undescribed taxa (Supplementary Table S1, available on Dryad). All major lineages were included (Tanaka et al. 1996; Veith et al. 2003; Hillis and Wilcox 2005; Che et al. 2007a; Matsui 2011). Based on other studies, the relationships of the unsampled species (Supplementary Table S2, available on Dryad) are uncontroversial and the species are distributed evenly across the tree. Thus, our sampling bias is negligible. Four species from *Odorrana*, *Pelophylax*, *Hylarana*, and *Rugosa* (Ranidae) were chosen as outgroup taxa based on Che et al. (2007b). New sequences from 80 species were analyzed, along with 14 species from GenBank (Veith et al. 2003; Hillis and Wilcox 2005; Che et al. 2007a) (Supplementary Table S1, available on Dryad).

DNA Extraction, Amplification, and Sequencing

We extracted DNA from muscle or liver tissues (either frozen or preserved in 95% ethanol) using standard phenol-chloroform extraction protocols (Sambrook et al. 1989). We amplified and sequenced three fragments of mitochondrial DNA (mtDNA) and six nuDNA loci (Supplementary Table S1, available on Dryad). The mitochondrial genes included 12–16S (partial sequence of 12S ribosomal RNA gene, complete sequence of $tRNA^{Val}$ and partial sequence of 16S ribosomal RNA), *CYTB* (cytochrome *b*) and *ND2* (partial sequence of NADH dehydrogenase subunit 2; complete sequence of $tRNA^{Ala}$, $tRNA^{Aln}$, $tRNA^{Trp}$; and partial sequence of the light strand replication origin). The nuDNA markers (Supplementary Table S3, available on Dryad) included *RAG1* (partial sequence of recombinase activating 1 protein gene), *RAG2* (partial sequence of recombinase activating 2 protein gene), *BDNF* (partial sequence of brain-derived neurotrophic factor gene), *SLC8A3* (partial sequence of solute carrier family 8 member 3), *TYR* (exon 1 of tyrosine precursor gene), and *POMC* (partial sequence of pro-opiomelanocortin A gene). We used standard polymerase chain reactions (PCRs) in 25-μμL reactions with the following protocol: initial denaturation step with 5 min at 95°C, 35 cycles of 94°C for 1 min, 41–57°C (depending on primers; Supplementary Table S3, available on Dryad) for 1 min, 72°C for 1 min and a single final extension at 72°C for 10 min. PCR products were purified with a Gel Extraction Mini Kit (Watson BioTechnologies, Shanghai). The purified product was used as the template DNA for cycle-sequencing reactions performed using BigDye Terminator Cycle Sequencing Kit (v2.0, Applied Biosystems). Sequencing was conducted on an ABI PRISM 3730 (Applied Biosystems) automated DNA sequencer. We sequenced amplified fragments with PCR primers in both directions and subjected the raw sequences to BLAST searches in GenBank to verify the amplifications.

Nucleotide sequences were aligned using ClustalX v1.81 (Thompson et al. 1997) with default parameters, and checked for ambiguously aligned regions in MEGA 5.0 (Tamura et al. 2011). Saturation tests for each gene and gene partitions were done using DAMBE (Xia and Xie 2001).

Phylogenetic Analyses

Bayesian inference (BI), maximum likelihood (ML), and maximum parsimony (MP) analyses were conducted using the nine concatenated gene fragments. BI analyses were performed in MrBayes v3.1.2 (Ronquist and Huelsenbeck 2003) using the optimal partitioning strategy and best-fit nucleotide substitution model for each region (Supplementary Table S4, available on Dryad) selected by PartitionFinder v1.1.1 (Lanfear et al. 2012). Four incrementally heated Markov chains (using the default heating value of 0.1) were run for 10 million generations each while sampling the chains at intervals of 1000 generations. Two independent runs were carried out. We discarded the first 50% of the samples as burn-in, and log-likelihood scores were tracked to assure convergence (effective sample size, ESS, values >200). We assessed topological convergence using AWTY (Nylander et al. 2008) to visualize the cumulative split frequencies in the set of posterior trees, as recommended by Moyle et al. (2012). The average split frequency value was set to <0.01 to assure convergence. The samples were summarized as a majority-rule consensus tree and the frequencies of nodal resolution were interpreted as Bayesian posterior probabilities (BPPs).

The ML trees were estimated using RAxML v7.0.4 (Stamatakis 2006). We used GTR+Γ as the substitution model, based on the partitioning strategy selected using PartitionFinder (Supplementary Table S4, available on Dryad). Support values were estimated from 1000 nonparametric bootstrap pseudoreplicates.

MP analyses were implemented using PAUP* 4.0b10a (Swofford 2003). The heuristic MP searches were executed for 1000 replicates using tree-bisection-reconnection branch swapping. All characters were treated as unordered and equally weighted. We used bootstrap analysis (BP) conducted with 1000 pseudoreplicates to assess nodal support. Gaps were treated as missing data.

We conducted exploratory BI analyses of a concatenated mitochondrial data set and a concatenated nuclear data to assess the separate contributions of each data type to the tree derived from all concatenated genes. We also conducted species tree estimation using the gene-tree-based coalescent methods ASTRAL (Mirarab et al. 2014) and MP-EST (Liu et al. 2010). We treated the three fragments of mtDNA as one locus, and the six nuDNA loci separately. For each of the seven loci, we generated 100 bootstrap replicates in RAxML v7.0.4 (Stamatakis 2006), and used the GTR+Γ model of sequence evolution. MP-EST analyses were conducted using the STRAW server (Shaw et al. 2013), and ASTRAL analyses conducted using ASTRAL v4.7.1 (Mirarab et al. 2014).

Divergence Times

Divergence times were estimated using BEAST v1.7.5 (Drummond et al. 2012) using a relaxed uncorrelated clock (Drummond et al. 2006). The substitution models and partitions were the same as used in the BI analyses. A Yule process was chosen for the tree prior. We used two independent analyses of 40 million generations each with sampling every 1000 trees. Convergence of the chains was determined with Tracer v1.5 (Rambaut and Drummond 2007), with target ESS values more than 200 for all parameters; 25% of samples were discarded as burn-in.

Nodes 2, 9, 5, and 17 (as shown in Fig. 1) were used for calibration. Node 2 was calibrated using a previous age estimate from Bossuyt et al. (2006; Fig. 3, their node 19). A normal prior distribution with mean of 31.2 and SD of 8.1 Ma yielded 2.5% and 97.5% quantiles of 15.3

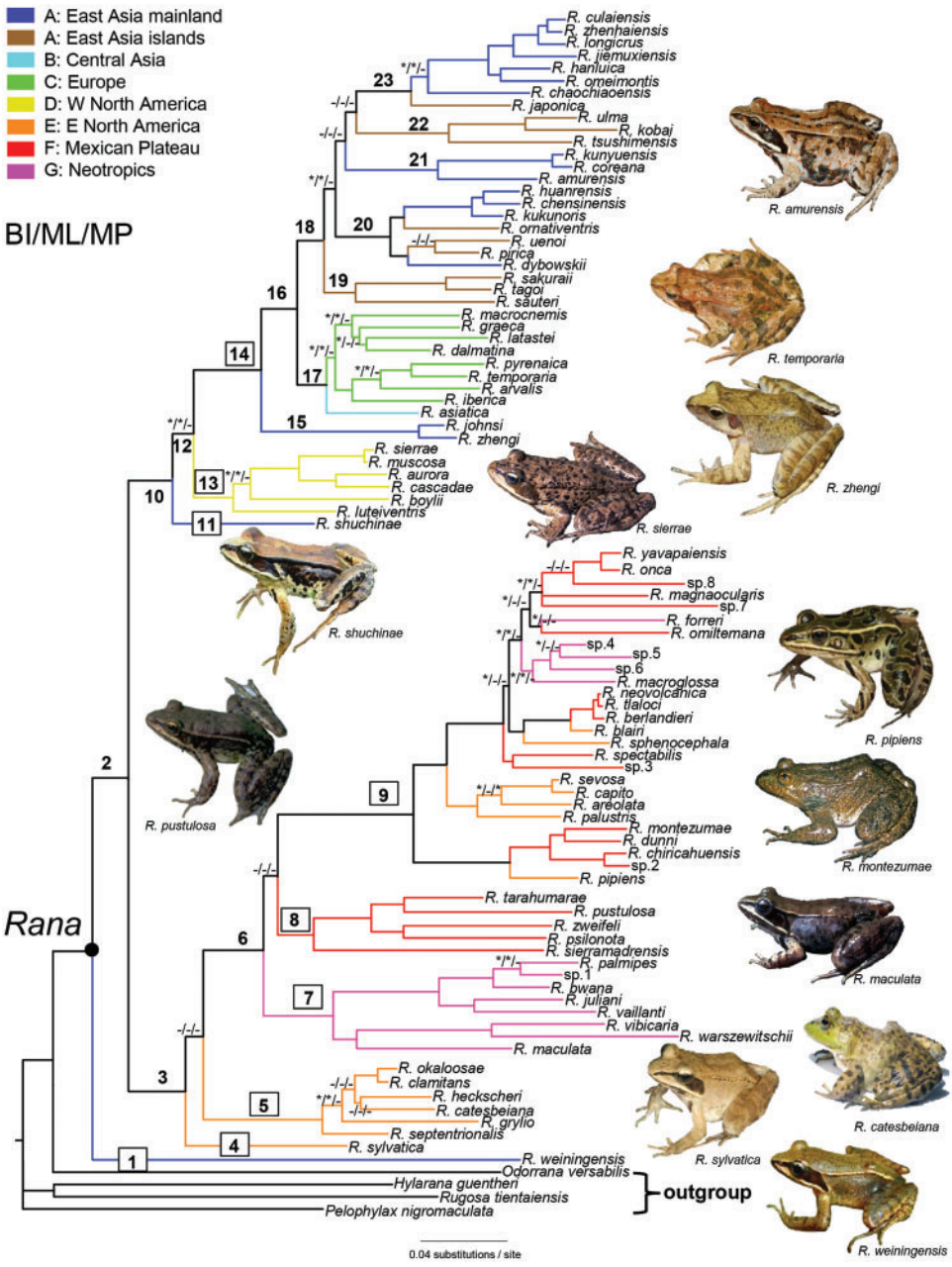

FIGURE 1. The BI tree derived from the combination of six nuDNA and three mtDNA loci. Branches without support symbols were strongly supported in all three phylogenetic analyses (BI, ML, and MP); we treated bootstrap proportions ⩾70% and BPPs ⩾95% as significantly supported (∗). Bootstrap proportions <70% and BPPs <95% were considered weakly supported (−). Support values are shown only for branches that were weakly supported in at least one of the three analyses, in which case support values are shown in order for BI, ML, and MP analyses. Colors of branches indicate the geographic distribution of extant taxa. Numbers on branches correspond to clades discussed in this study. Numbers with a black box correspond to the nine subgenera (plus *Rana sylvatica*) referred to in Supplementary Table S2, available on Dryad. Photographs depict the morphological variation of *Rana* across clades 1, 4, 5, 7, 8, 9, 11, 13, 15, 17, and 18. Frog illustrations are used with permission from David Hillis, Hui Zhao, Todd Pierson, Andreas Noellert, and Richard Sage.

and 47.1 Ma. Three node calibrations were based on fossil *Rana* representing the *R. pipiens* group (node 9), the *Rana catesbeiana* group (node 5), and the *R. temporaria* group (node 17). The last is based on a single articulated individual. The first two are represented primarily by ilia, one of the most commonly preserved elements of Tertiary fossil frogs. As noted by Parmley et al. (2010), it is relatively easy to diagnose *Rana* ilia from other genera due to the extremely prominent iliac crest. However, the ilia are less easily distinguished among species within *Rana*.

Assignment of the fossils to species groups by previous authors was based on overall similarity based on comparisons of several species of *Rana*. Because

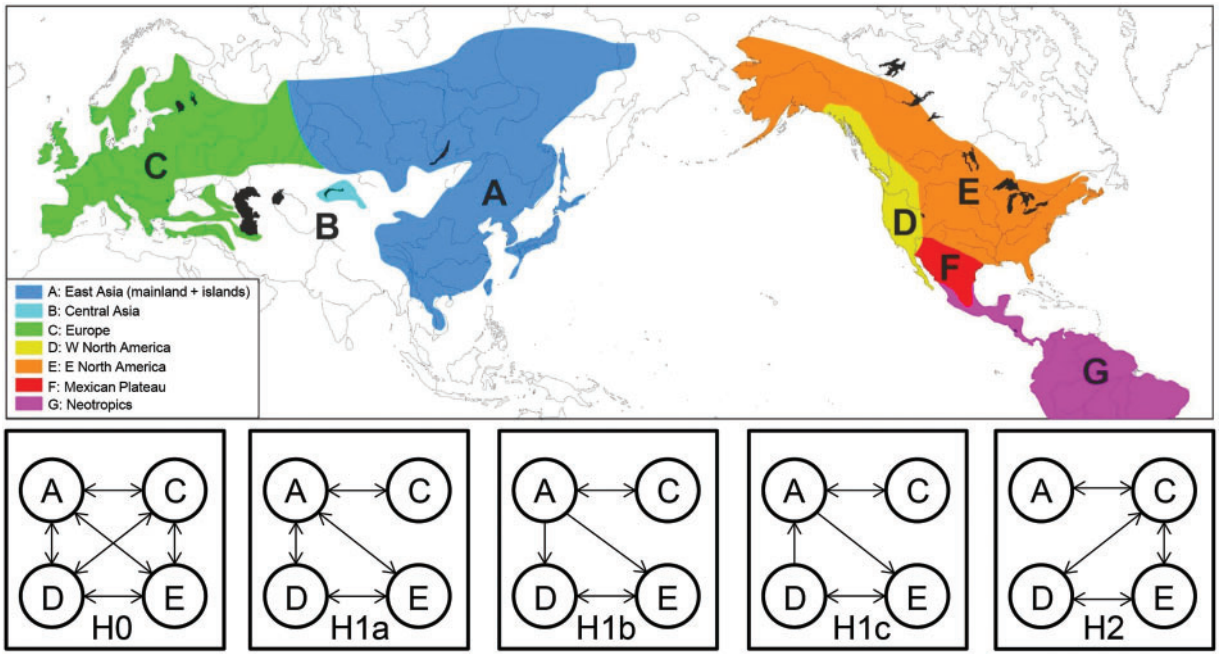

FIGURE 2. Map showing the generalized distribution areas of the extant *Rana* species and schematic drawings that illustrate possible dispersal events among the four major Holarctic areas under H0, H1, and H2. Seven major geographic regions (A–G) are indicated using colors. H0 is the null model, which assumes equal rates of dispersal between any two regions. H1 is the trans-Beringian hypothesis, which is further subdivided into H1a, with dispersals between East Asia and western North America and eastern North America, in either direction; H1b, two independent dispersals from East Asia to western North America and eastern North America (Macey et al. 2006); H1c, one dispersal from East Asia to eastern North America and one back to East Asia from western North America (Macey et al. 2006). H2 is the trans-Atlantic hypothesis: dispersal(s) occurred between Europe and western North America or eastern North America.

the authors explicitly allocated each fossil to a well-circumscribed clade of species, we inferred that the fossil is nested within that group, and used it to calibrate the most recent common ancestor (MRCA) of that group. The exception was the *R. temporaria* group fossil (see below).

We used a lognormal distribution to sample the prior for the age of each node. To parameterize the priors we used the BEAUTI user interface to set the "offset" as the minimum age of the fossil, the mean at 2.0 (standard scale), and the standard deviation at 1.0 (natural log). The mean and standard deviation were chosen so that the upper 97.5% quantile limit of each calibration age was 9–10 Ma older than the minimum age. Because no fossils that can be clearly allocated to *Rana* are older than 20 Ma, we view these limits as reasonable.

The calibration of node 9 was based on several "*Rana* cf. *Rana pipiens*" individuals from the Early Miocene Thomas Farm locality in Florida (18 Ma; Holman 1965, 1968). Holman concluded that the fossil ilia were not distinguishable from some extant species within the *R. pipiens* group (although they are from others), so we infer that the fossil is nested within the *R. pipiens* clade (node 9) and thus the clade had begun to diversify at least 18 Ma. The 2.5% and 97.5% quantiles of the prior distribution are 18.2 and 26.6 Ma.

Calibration of node 5 was based on Hottell Ranch Site fossils (15 Ma, Barstovian, Miocene), identified as *Rana* near *R.* "*clamitans*" (Voorhies et al. 1987), a species within the *R. catesbeiana* clade. Therefore, the MRCA of the *R. catesbeiana* group was calibrated at a minimum age of 15 Ma with 2.5% and 97.5% quantiles of 15.2 and 23.6 Ma. Voorhies et al. (1987) also identified "*R. pipiens* complex" ilia in their sample, suggesting that the authors were confident in the assignment of their *R. clamitans* fossil.

Calibration of node 17 was based on the single articulated fossil (*R. temporaria* group) from Dietrichsberg, Germany, dated at 19–20 Ma, early Miocene (Böhme 2001). Because the author did not state whether the fossil was nested within the *R. temporaria* clade, as opposed to being its sister species, we used it to calibrate the node immediately ancestral to the MRCA of the European clade; that is, the divergence of *Rana asiatica* from the European species of the *R. temporaria* group (node 17). We set the minimum age at 19 Ma; 2.5% and 97.5% quantiles are 19.2 and 27.6 Ma.

To test the sensitivity of our time calibration to particular calibration points, we used a jackknife analysis (Near et al. 2005). We successively deleted each of the individual fossil calibration points, repeated the calibration analyses, and compared the median age estimates with those ages from the complete analysis (Supplementary Table S5: Analyses 1–4, available on Dryad). Removing the *R. catesbeiana* group fossil yielded age estimates that were on average 8% younger than the estimates based on all fossil calibrations (Analysis 1). Similarly, removing the *R. temporaria* group fossil

(Analysis 4) yielded age estimates that on average were 9% younger than those of Analysis 1. In contrast, jackknife deletion of the *R. pipiens* group fossil (Analysis 3) yielded ages that were an average of 4% older than those of Analysis 1. Despite the modest systematic differences (older or younger) between the jackknife estimates and the complete analysis, the 95% credible intervals of the ages overlapped broadly, and so we used the calibration based on all fossils for our biogeographical analyses.

Biogeographic Multimodel Inference and Ancestral Range Estimation

To estimate the ancestral range for *Rana*, we defined seven major geographic regions (Fig. 2): (A) East Asia (mainland + islands), (B) Central Asia, (C) Europe, (D) western North America, (E) eastern North America, (F) Mexican Plateau and surrounding region, and (G) the Neotropics. We distinguished region B based on its arid continental climate and distinct anuran fauna compared with region A, and separated region C from regions A and B along the Ural Mountains and Caspian Sea, the area of the ancient Turgai Straits (Tiffney 1985a; Briggs 1995). We first divided the Americas into temperate and tropical regions, and then further divided North American temperate regions into eastern NA (E) and western NA (D) along the Rocky Mountains (Tiffney 1985b; Sanmartín et al. 2001; Donoghue and Smith 2004). We also defined an important transition area between the temperate and tropical regions that is centered on the Mexican Plateau (F), a hotspot of diversity in *Rana*. This region includes the montane areas of southern Arizona and New Mexico, from the Mogollon Rim southward, as well as the Edwards Plateau in Texas southward. The southern boundary of this region is defined by the montane regions of Mexico north of the Isthmus of Tehuantepec (Fig. 2). The Neotropics (G) lies south of this boundary, and along the lowlands of both the Atlantic and Pacific coasts. Areas A–C are collectively referred to as Old World, and D–G as New World.

We estimated model parameters and ancestral range probabilities using the DEC and DEC+J models in the BioGeoBEARS R package (Matzke 2013a; R Core Development Team 2014). The DEC model describes the temporal change in the range of a species, and distinguishes anagenetic change (between nodes) from cladogenetic change (at a node). It estimates two free parameters describing anagenesis: d, the rate of dispersal (range expansion) and e, the rate of extinction (range contraction) (Ree and Smith 2008). The DEC+J model includes a third parameter, j, which describes the relative weight of founder event speciation during cladogenesis (Matzke 2013b). Under this model, which resembles founder event speciation, an ancestor in area A instantaneously "jumps" to area B, leaving one descendant in A and one in B. An increase in j reduces the weight of the traditional DEC cladogenesis processes.

We followed the terminology of Matzke (2014) for cladogenetic events. Vicariance is the splitting of a species' range such that the two descendants have non-overlapping ranges. In sympatric-subset cladogenesis, the range ABC yields two descendant ranges that overlap, such as (ABC, A), or (ABC, B). In sympatric range-copying cladogenesis, the ranges of each descendant node are identical with their ancestor.

To test the hypotheses of intercontinental dispersal, we used dispersal matrices (Supplementary Table S6, available on Dryad) to indicate the probability of dispersal events between two areas. We first performed an unconstrained analysis, assuming equal probability of dispersal among all adjacent areas (Fig. 2), as our null model (H0) to compare to hypotheses of Trans-Beringian (H1) and the Trans-Atlantic dispersals (H2).

Under the Trans-Beringian hypothesis (H1), we considered (a) dispersals only between East Asia and western NA and eastern NA, in either direction; (b) two independent dispersals from East Asia to western NA and eastern NA (Macey et al. 2006); and (c) one dispersal from East Asia to eastern NA and one back to East Asia from western NA (Macey et al. 2006). Under the Trans-Atlantic hypothesis (H2), we tested whether dispersal(s) occurred between Europe and western NA or eastern NA.

We assigned a value of 1 for unrestricted dispersal between two areas and 0.001 for disallowed dispersal (0.0 causes computational difficulties; Supplementary Table S6, available on Dryad). For all analyses the maximum number of areas was set at four. We specified allowed connections with an area adjacency matrix (Supplementary Table S7, available on Dryad). The fit of all models to the data was compared using AIC, and the combination of connectivity model (dispersal matrices) and DEC/DEC+J was determined using relative model weights (Supplementary Table S9, available on Dryad).

The ML estimates for each model were then used to calculate the ancestral range probabilities at each node of the tree. Given that all species of *Odorrana*, the immediate outgroup of *Rana* (Che et al. 2007b; Stuart 2008), occur in East Asia, we fixed the node below *Rana* to have an East Asian distribution using the BioGeoBEARS "fixlikes" option in all analyses.

Diversification Patterns

Diversification analyses used (1) the entire genus *Rana*, and (2) subsets of species within a region of interest. We used the R package *ape* (Paradis et al. 2004) to generate a lineage-through-time (LTT) plot based on the maximum clade credibility tree and 95% credible interval obtained by random sampling of 1000 trees from the post-burnin posterior distribution of the BEAST analysis using Burntrees v.0.1. (http://www.abc.se/~nylander/). Outgroups were excluded. In addition, we explored regional diversification of *Rana* using scripts provided by Mahler et al. (2010) to visualize the accumulation of lineages within different regions. These differ from LTT plots in that they reflect diversity due to both *in situ* diversification and independent immigration events (see McGuire et al. 2014).

We performed four LTT analyses to explore regional patterns of diversity. First, we compared Old World and New World species. Second, we compared individual regions: East Asia, Europe (including central Asia considering their close relationships), western NA, and eastern NA. Third, we partitioned the East Asia region into mainland and islands to examine the contribution of species from East Asian islands, for example, Japan and Taiwan. Last, we compared western NA, eastern NA, the Mexican Plateau, and the Neotropics to identify which regions contributed the lineage accumulation in clade 3 (Fig. 1).

Because the LTT plots measure only the accumulation of species and not speciation/extinction rates, we used BAMM (Rabosky 2014) and MEDUSA (Alfaro et al. 2009) to examine diversification rate heterogeneity along the branches. Analyses were conducted using three groups: all *Rana*, Old World *Rana* (Fig. 1: clades 1 + 11 + 14), and New World *Rana* (using clade 3 only, because clade 13 represents an independent dispersal into the New World).

The BAMM analyses used 200 million generations, sampling every 10,000 generations, and sampling event data every 10,000 generations. We simulated the prior distribution on the number of rate shifts. The effect of unsampled taxa was determined by using a nonrandom incomplete taxon-sampling correction. We removed the first 30% of generations as burn-in after checking MCMC convergence using BAMMtools (Rabosky et al. 2013; Rabosky 2014). We checked the ESS (target value of 300) using the CODA package (Plummer et al. 2006). The final results, including the credible set of rate shifts, the best shift model, and rate-through-time curves, were summarized and visualized using BAMMtools.

We also estimated speciation/extinction rates using MEDUSA, part of the R package *geiger* (Harmon et al. 2008). The former fits a birth–death model to the phylogeny (Alfaro et al. 2009) and detects significant rate shifts along the branches. We ran analyses using the default AIC threshold. The MEDUSA algorithm first estimates likelihood and AIC scores with the simplest birth–death model (two parameters, b and d). Then, it compares the AIC scores of this model with an incrementally more complex model that includes five parameters (two birth parameters and two death parameters owing to one break point and a shift-location parameter). This process is terminated when further addition of parameters does not improve the AIC score.

Results

Phylogenetic Analysis

Our final data set included 94 sequences from 12S–16S; 70 from *CYTB*; 69 from *ND2*; 76 from *RAG1*, *RAG2*, *BDNF*, and *SLC8A3*; and 77 from *POMC* and *TYR*, plus sequences downloaded from GenBank (Supplementary Table S1, available on Dryad). Seventy-seven species included both mtDNA and nuclear sequences, whereas 17 species had GenBank mtDNA sequences only; tissues were not available for additional analysis. For the 77 taxa with both nuclear and mtDNA data, some samples were not successfully amplified for all genes, including four from *CYTB*; six from *ND2*; and one from each of *RAG1*, *BDNF*, and *SLC8A3*. We deposited the 639 new sequences in GenBank (No. KX269176–KX269814).

The final matrix consisted of 7250 positions, including 1849 parsimony-informative sites (Supplementary Table S4, available on Dryad). We translated all protein-coding gene sequences into amino acids to check for stop codons. In the fragment of 12S–16S and *POMC*, regions of ambiguous alignment were excluded. No indication of a saturation effect was detected (Supplementary Table S8, available on Dryad). The preferred substitution models for each partition are listed in Supplementary Table S4, available on Dryad.

The BI, ML, and MP trees were very similar (Fig. 1 and Supplementary Fig. S1, available on Dryad). The main conflict between mtDNA and nuclear genes involved the position of *Rana sylvatica* and the relationships among the three major New World groups within clade 6 (Supplementary Fig. S2, available on Dryad). Our species-tree analyses (Supplementary Fig. S3, available on Dryad) produced results that were consistent with our concatenated analyses (Fig. 1), but with somewhat less resolution. Given the greater resolution of the concatenated analysis, and its general agreement with the species-tree analysis, we used the concatenated analysis for our biogeographic assessment (Figs. 1 and 3). Our analyses resolved the following seven major geographic lineages of *Rana* with strong support: *Rana weiningensis* (clade 1) from southwestern China was the sister group of the remaining taxa, which together included a New World clade 3 (eastern North America, Mexican Plateau, and Neotropics), southwestern China (clade 11; only *Rana shuchinae*), western North America (clade 13), southwestern China and northern Vietnam (clade 15), Central Asian *R. asiatica* plus Europe (clade 17), and East Asia (clade 18), including the mainland and adjacent islands.

We found that species of Old World *Rana* are paraphyletic with respect to the two New World clades. The major well-differentiated, morphologically and ecologically distinct clades within New World *Rana* largely support the traditional subgeneric designations for the genus (Dubois 1992; Hillis and Wilcox 2005; Hillis 2007; AmphibiaWeb 2015). The New World clade 13 consists of the *Rana boylii* group in western North America (the subgenus *Amerana*). The second New World clade (clade 3) includes the remaining North and South American taxa, with five strongly differentiated subclades (Fig. 1): *R. sylvatica* (clade 4), which forms the sister group of the remaining species; the *R. catesbeiana* group (clade 5; the subgenus *Aquarana*); the *Rana palmipes* group (clade 7; the subgenus *Lithobates*, although that subgenus was further subdivided by Hillis and Wilcox 2005); *Rana sierramadrensis* plus the *Rana tarahumarae* group (clade 8; the subgenus *Zweifelia*, although that name was used for the *R. tarahumarae* group alone by Hillis and Wilcox 2005); and the *R. pipiens*

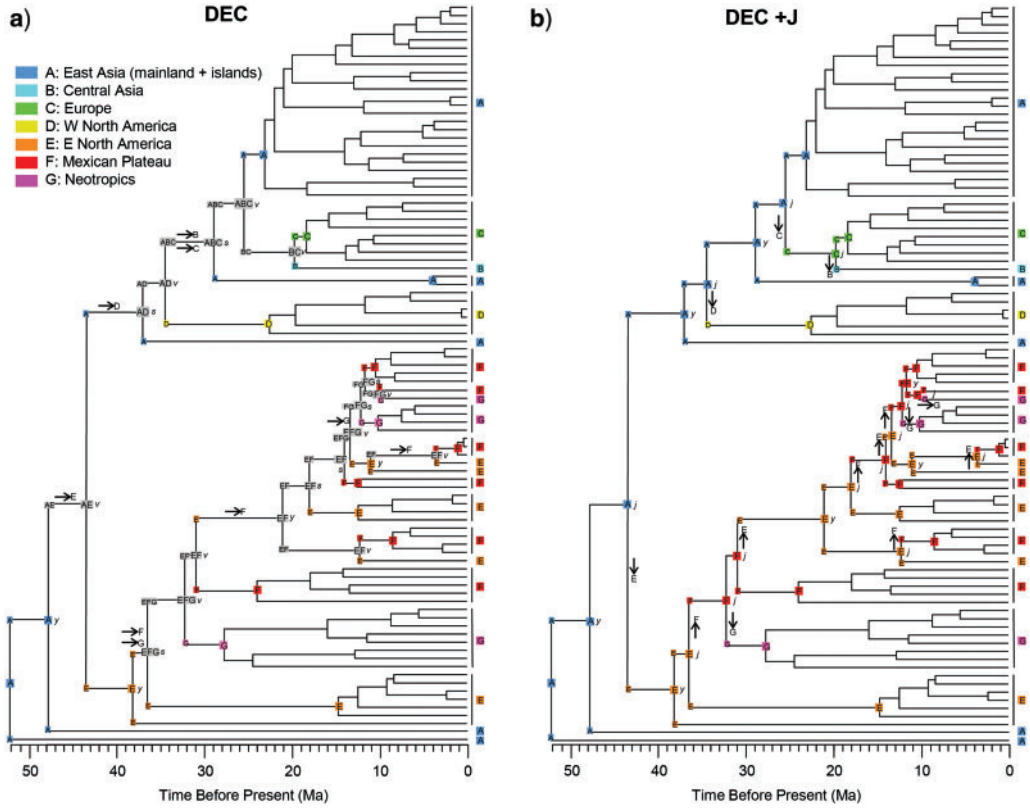

FIGURE 3. Spatiotemporal reconstruction of the true frogs based on the Trans-Beringia hypothesis (H1b). Results based on the (a) DEC and (b) DEC+J likelihood methods implemented in BioGeoBEARS are presented. The tree topology, derived from BEAST analyses, is consistent with the Bayesian tree of Figure 1. Branch lengths are proportional to divergence times. Means and 95% confidence intervals of divergence times are presented in Supplementary Figure S5, available on Dryad. Colors reflect biogeographic designations (for species at tips) and most probable states at each node. Gray colors indicate nodes with multiple ancestral states. States at nodes represent the most probable ancestral area before the instantaneous speciation event, whereas those on stems represent the state of the descendant lineage immediately after speciation. Some node and stem labels are omitted to reduce clutter; in all cases these are identical to the state at both the ancestral and descendant nodes. The corresponding pie charts for the proportional likelihoods of ancestral area states at each node and stem are presented in Supplementary Figure S6, available on Dryad. Abbreviations: *y*, sympatric range-copying speciation; *s*, sympatric-subset speciation; *v*, vicariance; *j*, jump-dispersal or founder event speciation. Arrows show the dispersal events.

group (clade 9; the subgenus *Pantherana*). Although each of these distinct groups is strongly supported, the higher relationships among groups have weaker support.

The East Asian taxa (clades 1, 11, 15, and 18) formed a polyphyletic group. Clade 18 included five well-supported subclades (Fig. 1 and Supplementary Fig. S4, available on Dryad): clades 19 and 22 included exclusively the East Asian species from Taiwan and Japan; 20, 21, and 23 included the remaining insular species and closely related taxa from the East Asian mainland. The unresolved relationships among the five subclades suggest rapid radiation.

Divergence time estimates from the BEAST chronograms are shown in Figure 3 (with details in Supplementary Fig. S5, available on Dryad). These are described in concert with the historical biogeography below.

Historical Biogeography

The DEC+J class of models always conferred a much higher likelihood on the data than DEC (log-likelihood differences of 11–16 units; Supplementary Table S9 and Supplementary Fig. S6, available on Dryad). Within each class, all submodels that allowed dispersals across Beringia (H1) were favored over the Trans-Atlantic dispersal hypothesis (H2) (Supplementary Table S9, available on Dryad). Among the Beringian dispersal hypotheses, hypothesis H1b (two independent dispersal events from East Asia to North America) received the strongest support. Thus, we used this model in our evaluation of ancestral range estimates.

We contrasted the results of the DEC and DEC+J models (Fig. 3) under hypothesis H1b. DEC (Fig. 3a) estimated the dispersal rate (*r*) as 0.0023 and the extinction rate (*e*) as 0.0. By definition, the jump-dispersal rate (*j*) was 0.0 under this model. We identified nine dispersal events (horizontal arrows on Fig. 3a). In almost all cases, these were followed by a vicariance event (*v*) that split the ancestral range. We inferred 10 vicariance and 7 sympatric-subset events (*s*). The remaining events we inferred were sympatric range-copying events, in which the ranges of both descendants were identical to

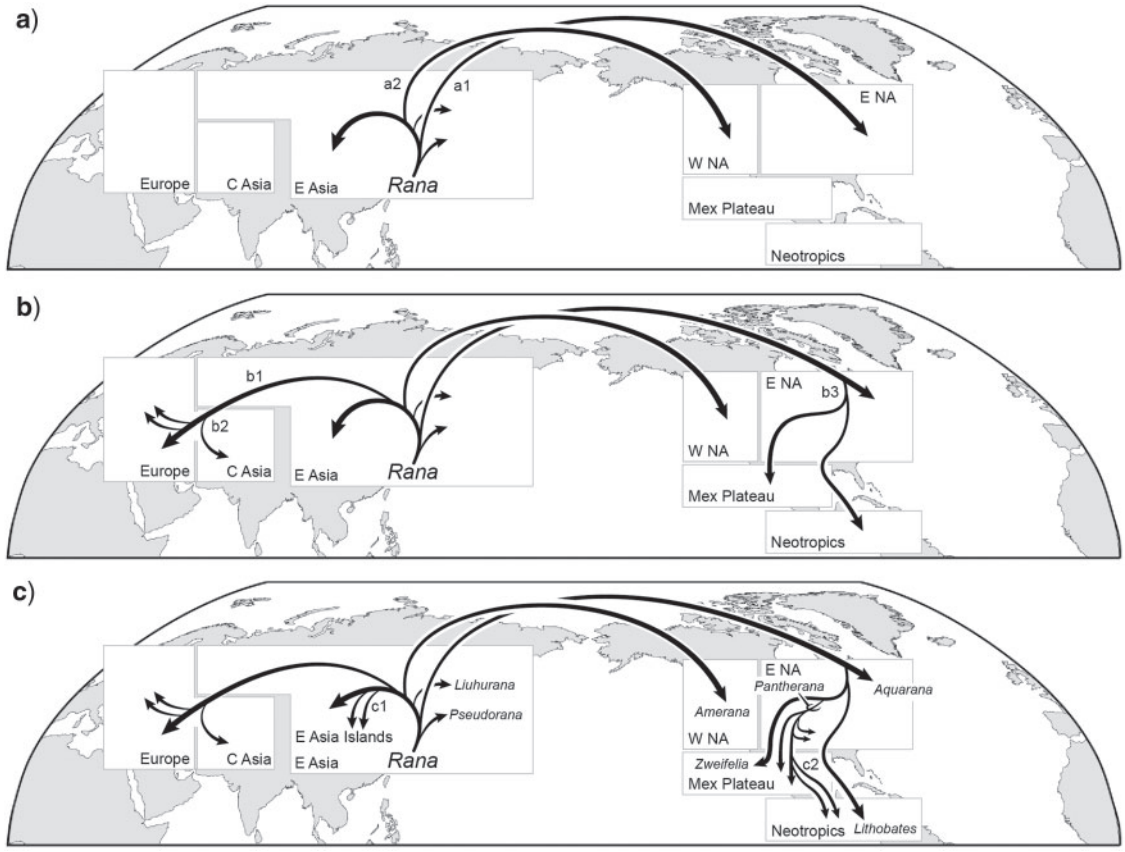

FIGURE 4. Summary of major range shifts (dispersal and vicariance) of *Rana* over three time periods (a–c). For details of the range shifts see Figure 3. (a1) Dispersal to eastern North America within the interval 48–43 Ma, followed by vicariance at 43 Ma. (a2) Dispersal to western North America 43–34 Ma, followed by vicariance at 34 Ma. (b1) Dispersal to Europe + Central Asia (composite area) during 29–25 Ma (or possibly earlier; see text). (b2) Europe and Central Asia split at 20 Ma by vicariance. (b3) Dispersal to the Mexican Plateau + Neotropics composite area during 37–32 Ma; the Neotropics split from its sister-group (eastern North America + Mexican Plateau clade) by vicariance at 32 Ma; divergence at 31 Ma of the first of several Mexican Plateau clades. (c1) Repeated dispersals among East Asia Islands and the mainland during 20–5 Ma. (c2) At least two dispersals from the Mexican Plateau to the Neotropics during 13–10 Ma. Taxon names in panels are subgenera.

those of the ancestor (y); most of these are not shown to avoid visual clutter.

We focus first on the divergences of the earliest-diverging branches. Under the DEC model (Fig. 3a), range expansions can be described by a combination of dispersal followed by vicariance or sympatric-subset events. Because the reconstruction of areas at some nodes is not definitive, we report general patterns rather than enumerating each event.

The MRCA of *Rana* dated to the Eocene at about 48 Ma (95% credibility interval [CI]: 55–40 Ma). The first dispersal involved a range expansion through Beringia and then across high latitudes of North America into eastern North America about 48–43 Ma (Fig. 4a), followed by vicariance at 43 Ma resulting in an eastern North American clade 3 and an Asian clade 10 whose ancestral range is reconstructed as East Asia (Area A). The latter then underwent a second range expansion across Beringia and then south into western North America 43–34 Ma (Fig. 4a), followed by vicariance (node 12) at 34 Ma, yielding a western North American clade (13) and a clade of Eurasian species (clade 14). The Eurasian clade subsequently split into an East Asian clade and a clade in Europe and Central Asia (Fig. 4b). The East Asian lineage continued to diversify into a series of lineages, some of which dispersed into the East Asian islands (the Japanese islands, Sakhalin, the Kurils, and Taiwan; Supplementary Fig. S4, available on Dryad, and Fig. 4c).

In the New World radiation, the first invasion of *Rana* from Asia underwent a primary split into two lineages: *R. sylvatica* versus the remaining species. Then another split occurred among the majority of species between clade 5 (*Aquarana*; the North American water frogs) and a clade that expanded into the Mexican Plateau and the Neotropics (Fig. 4b). Shortly thereafter (~32 Ma), this latter clade split to form clade 7 (*Lithobates*; the Neotropical true frogs), and in turn a second lineage split at approximately 31 Ma, yielding clade 8 (*Zweifelia*; the torrent frogs) on the Mexican Plateau, and the large clade 9 (*Pantherana*; the leopard frogs; Fig. 4c). Within *Pantherana*, two lineages, *R. forreri*, and a clade comprising *R. macroglossa*, sp. 4, sp. 5, and sp. 6, diverged from their close relatives at approximately 11

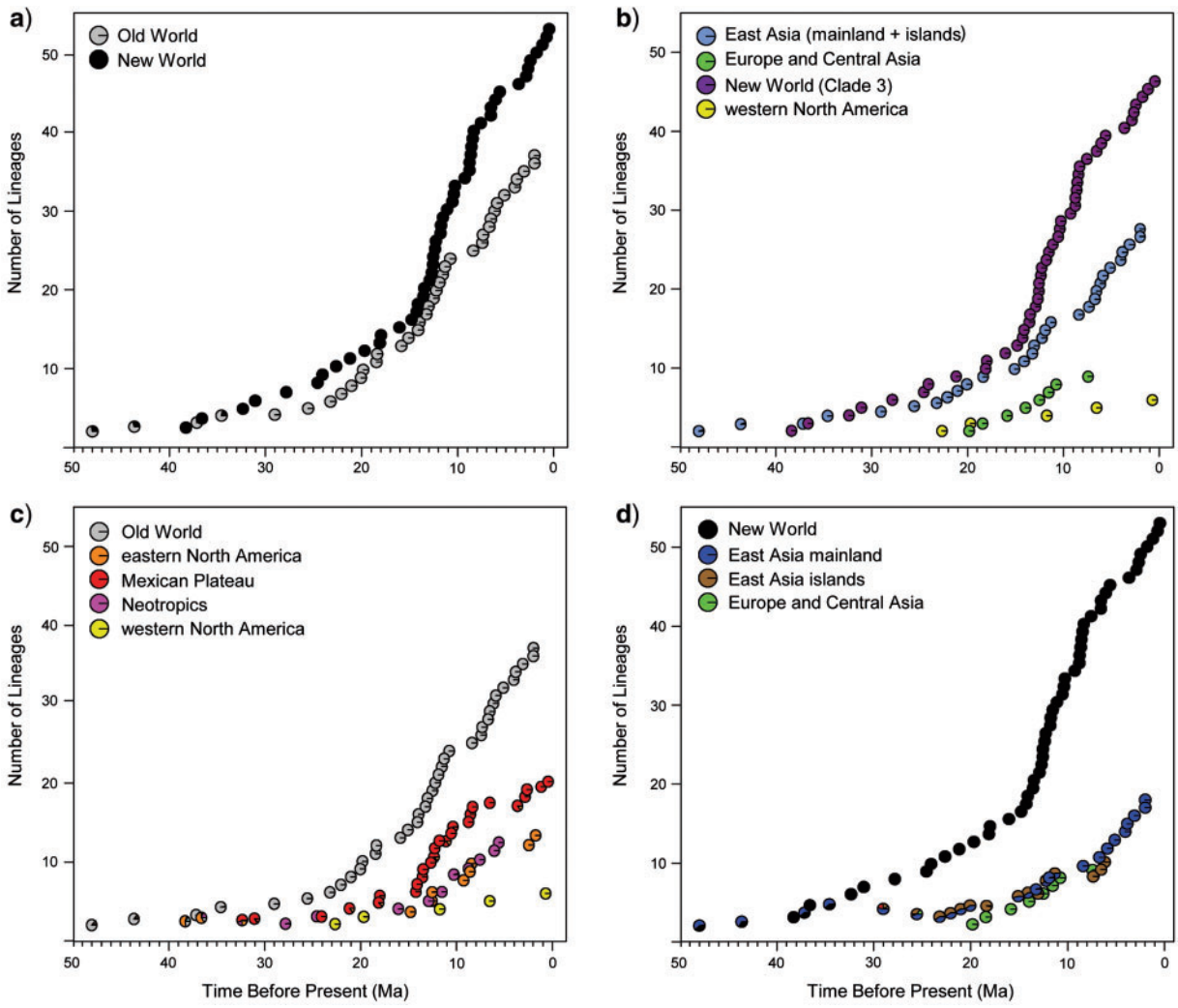

FIGURE 5. *Rana* species accumulation curves as estimated for regions: (a) the Old World (clades 1, 11, and 14; see Fig. 1) and New World (clades 3 and13); (b) East Asia (mainland + islands, clades 1, 11, 15, and 18), Europe and Central Asia (clade 17), the New World (clades 3 and 13); (c) Old World, eastern North America, western North America, Mexican Plateau and surrounding region, and Neotropics; (d) New World, East Asia mainland, East Asia islands, Europe and Central Asia. The *y*-axis and *x*-axis show the historical lineage diversity estimates and relative branching times obtained from the time-calibrated phylogeny, respectively. Pie charts are color-coded to reflect the proportional likelihoods of alternative ancestral state reconstructions.

Ma to occupy the Neotropics. The remaining species of *Pantherana* are found in eastern and northern North America and the Mexican Plateau. In contrast, clade 13 (*Amerana*) gave rise to several species beginning at 23 Ma, but none of the descendants expanded east or south into other areas. Ambiguities of ancestral range estimation (Fig. 3) make precise interpretation of the biogeographic history difficult, but at least four dispersal/vicariance events occurred between eastern North America and the Mexican Plateau.

Under the DEC+J model (Fig. 3b), these patterns can be explained by 14 jump dispersals (*j* symbol at the node, and vertical arrows). The *j* parameter was estimated to be 0.0279, and *d* and *e* were 0.0. Under this model, no vicariance events are inferred. We inferred seven sympatric range-copying cladogenetic (*y*) events, but no sympatric-subset cladogenetic events. Although the estimated ranges and inferred mechanisms differed, the locations of range shifts on the tree were similar under both models.

Diversification Patterns

The standard LTT plot for all *Rana* depicted a near-constant accumulation of lineages through time until about 12 Ma, after which there was a gradual slowdown (Supplementary Fig. S7, available on Dryad). However, diversification plots of regions (Fig. 5) indicated several region-specific patterns.

Generally, the Old World species (Fig. 1, clades 1 + 11 + 14) show a different trajectory of lineage accumulation compared with taxa of the New World (Fig. 1, clade 3 + 13) (Fig. 5a). Further regional plotting indicates that East Asian clades 1 + 11 + 18 and the larger clade 3 from

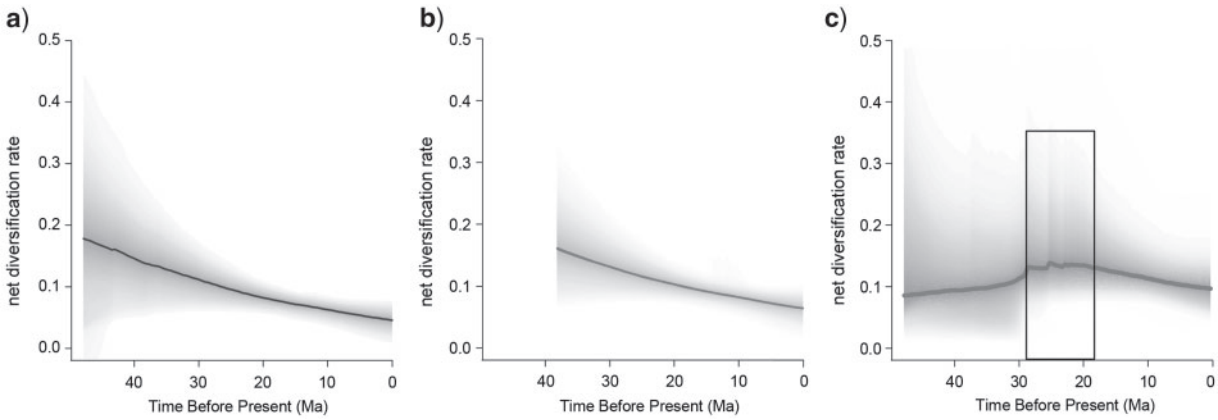

FIGURE 6. Temporal dynamics of diversification rate through the evolutionary history of *Rana* revealed by BAMM analyses. Rate-through-time curves depict clade-specific net diversification trajectories for (a) all *Rana* species, (b) the New World clade 3, and (c) the Old World species (clades 1, 11, and 14; Fig. 1). Shading intensity reflects relative probability of a given diversification trajectory, with upper and lower bounds denoting the 90% Bayesian credible interval on the distribution of rates through time. A period of elevated diversification rate in (c) is highlighted by a rectangle.

eastern NA, the Mexican plateau, and the Neotropics are important in explaining the diversity of the Old World and New World, respectively (Fig. 5b). The Old World *Rana* began species accumulation about 48 Ma ago, slowly at first, until 29 Ma; this was followed by continuous cladogenesis, and acceleration of the rate of lineage accumulation (Fig. 5a). Plots of the East Asian lineages (Fig. 5b,d) indicate that East Asian islands account for a substantial portion of Old World *Rana* diversity, especially given the small size of the islands relative to the mainland.

Generally, lineage accumulation in the New World showed a faster rate than in the Old World (Fig. 5a,b), and especially an increase in the rate of cladogenesis around 14 Ma. This increase is associated with separate radiations in eastern North America, the Mexican Plateau, and the Neotropics, of which the radiation on the Mexican Plateau had the greatest impact (Fig. 5c). In contrast, species accumulation in western North America was relatively slow and constant, resulting in only eight extant species after the second dispersal from East Asia (Fig. 5b).

Unlike the regional LTT analyses, BAMM analysis of all *Rana* indicated an initial high net diversification rate that gradually decreased through time (Fig. 6a and Supplementary Figs. S8a and S9a, available on Dryad). Analyses further supported strongly heterogeneous diversification dynamics between the Old World and New World species (Fig. 6 and Supplementary Figs. S8b,c and S9b,c, available on Dryad). The pattern for the New World species (clade 3) supports diversity-dependent speciation, with a pattern of initial high diversification that gradually decreased through time (Fig. 6b). In contrast, both BAMM and MEDUSA analyses detected a more sudden rate shift among the Old World species (Fig. 6c and Supplementary Figs. S8c, S9c, and S10, available on Dryad). The net diversification rate from BAMM shows a hump-shaped curve for the Old World species, with an increased rate from 29 to 18 Ma (about 0.14 species/Ma; Fig. 6c). The MEDUSA analysis also suggested that the current diversity of Old World *Rana* (clades 1 + 11 + 14) is best explained by one rate shift (AICc threshold = 2.01; Supplementary Fig. S10, available on Dryad); the average speciation rate increases significantly from 0.013 to 0.093 after the split of *R. shuchinae* from other *Rana* at approximately 37 Ma.

DISCUSSION

Phylogeny and Classification of Rana

Our analyses yield a comprehensive and well-resolved phylogeny for the genus *Rana* and strongly confirm its monophyly. Our treatment of *Rana* is largely consistent with that used by AmphibiaWeb, except that *R. cangyuanensis* is now considered part of *Odorrana* (Fei et al. 2012). Previous studies have been hampered by sampling restricted geographic regions or limited species groups with limited gene markers, mostly based on mtDNA analyses (e.g., Tanaka et al. 1996, Tanaka-Ueno et al. 1998; Veith et al. 2003; Hillis and Wilcox 2005; Frost et al. 2006; Che et al. 2007a; Matsui 2011). In contrast, our tree is based on deep taxon sampling and multiple nuclear and mitochondrial loci. Prior studies did not recover most of the phylogenetic relationships because they did not simultaneously consider both Eurasian and American species.

The two New World clades of *Rana* (3 and 13 in Fig. 1) clearly nest within East Asian clades (1, 11, 15, and 18 in Fig. 1), and thus the simple sister pairs of intercontinental disjunct *Rana* lineages (e.g., Macey et al. 2006) cannot be assumed. This finding for *Rana* mirrors the conclusions of Wen (1999), who considered similar intercontinental distributions of several plant groups, and found that many taxa traditionally treated as disjunct sister groups were polyphyletic or paraphyletic. Our study highlights the importance of thorough sampling for phylogenetic history constructions.

The phylogenetic relationships we recovered do not support some of the taxonomic assignments suggested by Fei et al. (2012) and Frost (2015) (Supplementary Table S2, available on Dryad). For example, *Pseudorana* from both Fei et al. (2012) and Frost (2015) is paraphyletic. Clade 15 contains *Rana johnsi*, *Rana zhengi*, and *Rana sangzhiensis* (Fig. 1 and Jing Che unpublished data) and these are not the sister taxa of clade 1 (*R. weiningensis*).

Morphological homoplasy has led to some of the taxonomic confusion surrounding the genus *Rana*. The presence of grooves on the toe pads of adults in the species in clades 1, 15, and *Rana sauteri* (within clade 19), and an abdominal sucker in the tadpole of *R. sauteri*, have led to various taxonomic proposals for these species. For example, *Pseudorana* (Fei et al. 1990) and *Pseudoamolops* (Jiang et al. 1997) were established as separate genera but with various compositions of species (Dubois 1992; Ye et al. 1993; Fei et al. 2012). The recognition of *Pseudoamolops* has long been rejected by phylogenetic studies (e.g., Tanaka-Ueno et al. 1998; Che et al. 2007a, 2007b) and our results corroborate these findings. Frost et al. (2006) included both *Pseudorana* and *Pseudoamolops* in *Rana*, and at the same time, recognized clade 3 of this study as *Lithobates* based on limited species and gene sampling. However, that arrangement makes the remaining *Rana* paraphyletic. Later, largely based on the phylogeny of Che et al. (2007b), Frost (2015) revived the use of *Pseudorana* and recognized genera *Pseudorana*, *Lithobates*, and *Rana* as the three genera of "true frogs". However, this action still does not result in entirely monophyletic taxa (Supplementary Table S2, available on Dryad).

Even if these groups were fixed by transferring species among these taxa, the major morphological, ecological, and behavioral differentiation within *Rana* does not occur among these poorly differentiated taxa (*Pseudorana*, *Rana*, and *Lithobates* sensu Frost 2015), but within them. For example, biologists have a much greater need for names of well-differentiated groups including *Pantherana* (the leopard frogs), *Zweifelia* (the torrent frogs), *Lithobates* (the Neotropical true frogs), and *Aquarana* (the North American water frogs), than for a taxon that combines these groups. Hillis and Wilcox (2005) provided nested, clade-based names at both levels, but Dubois (2006) argued that such nested subgeneric names were incompatible with the rules of the International Code of Zoological Nomenclature (ICZN). Hillis (2007) disagreed with Dubois' interpretation of the ICZN rules, but nonetheless suggested a compromise classification that recognized the distinct, nonoverlapping clades within *Rana* as subgenera.

Based on our phylogenetic analyses and the lack of any diagnostic morphological characters for the putative genera recognized by Fei et al. (2012) or Frost et al. (2006), and the clear monophyly of the larger group, we retain all these species in the traditional genus *Rana* (Supplementary Table S2, available on Dryad). This also has the desirable outcome of retaining the traditional binomial species names for these well-studied species, and thus retaining the connections of these names to their corresponding extensive literatures.

We support the recognition of the major diverse lineages within *Rana* (the groups that show significant molecular, morphological, ecological, and behavioral divergences) as subgenera (Supplementary Table S2, available on Dryad), which largely match the traditional major distinct species groups long recognized by numerous authors (Zweifel 1955; Case 1978; Farris et al. 1980, 1983; Hillis et al. 1983, 1984; Hillis 1988, 2007; Hillis and de Sá 1988; Dubois 1992; Hillis and Wilcox 2005). The subgenera of *Rana* are *Pseudorana* (clade 1), *Aquarana* (clade 5), *Lithobates* (clade 7), *Zweifelia* (clade 8), *Pantherana* (clade 9), *Liuhurana* (clade 11), *Amerana* (clade 13), and *Rana* (clade 14) (Fig. 1, Supplementary Table S2, available on Dryad).

The inferred relationships of *R. sylvatica* differed in the trees derived from nuclear versus mitochondrial genes (Supplementary Fig. S2, available on Dryad), and different studies and data sets have placed this species at various places within clades 3 and 10 (Case 1978; Farris et al. 1980, 1983; Post and Uzzell 1981; Hillis and Davis 1986; Hillis and Wilcox 2005). In our combined analysis, *R. sylvatica* forms the sister group of all the other remaining New World *Rana* (Fig. 1), which is consistent with Case (1978) based on immunological data. However, the support is weak (Fig. 1), because mtDNA sequences conflict with the signal from the six nuclear genes regarding the placement of *R. sylvatica* (Supplementary Fig. S2a,b, available on Dryad). The different resolutions for this species may indicate hybridization or incomplete lineage sorting among the ancestral lineages of clade 3.

Biogeographic Processes Inferred from DEC and DEC+J Models

The DEC model most often interprets range evolution as expansion into an unoccupied area (i.e., dispersal) (Matzke 2014), followed by splitting of the ancestral range by vicariance or sympatric-subset cladogenesis into two daughter species with more restricted ranges. In total, nine dispersals followed by 10 vicariance speciation and 7 sympatric-subset events were inferred, for a total of 16 range changes under DEC compared with 14 under DEC+J. In some cases, even though DEC and DEC+J reconstructed the same number of changes in ancestral range, the interpretation (e.g., dispersal vs. vicariance) may differ because of differences in the models.

Although the DEC+J model was significantly favored over DEC under all scenarios, it is worth considering its suitability for this analysis given that it was developed to accommodate founder event speciation (*j* parameter), which is common in oceanic island systems (Matzke 2014). Under DEC+J, the ancestral ranges of all nodes involve a single area (Fig. 3b). Pie charts of the relative likelihoods of alternative reconstructions (Supplementary Fig. S6c4, available on Dryad) showed low likelihoods, except for ancestral

node 17. This suggests that founder event speciation was more common than vicariance or sympatric-subset speciation.

In contrast, DEC range reconstructions include 18 nodes with >1 area (not including the "corner" nodes). These reflect classic dispersal into new regions. The reconstructions for several nodes are ambiguous, having alternative possibilities with similar likelihoods.

The DEC+J model typically yields higher overall likelihood scores and the range estimates are unambiguous, as expected (Matzke 2013b, 2014). Thus, DEC+J presents a "cleaner" scenario. However, it is worth considering whether the DEC+J model is biologically meaningful to dispersal between contiguous areas within a continent. An improvement in likelihood score indicates a better fit of data to a particular model only, which does not mean that the model offers a better biological explanation for the data. Notwithstanding, the DEC class of analyses also may be biased depending on how the distributional data were scored. Matzke (2014) pointed out that in his simulations DEC+J tended to be favored in trees with terminal taxa that occupied a single area, whereas DEC was favored when terminal taxa occupied multiple areas. Because we assigned all terminal taxa to a single area, the favoring of DEC+J is not surprising. Clearly, the choice of terminal assignment to one or more areas may affect model selection.

Historical Biogeography

The origin and evolution of *Rana* has been of long-standing interest to systematists and biogeographers (e.g., Case 1978; Veith et al. 2003; Macey et al. 2006). Our extensive sampling suggests that *Rana* originated in the East Asia region, perhaps in southwestern China (Figs. 1 and 3) where three distinct, well-differentiated groups occur: *R. weiningensis* (clade 1), *R. shuchinae* (clade 11), and the sister species *R. zhengi* and *R. johnsi* (clade 15) (Fig. 1). The former two species have limited distributions at high elevations on the Yunnan-Guizhou Plateau (1700–2950 m and 2760–3800 m, respectively). Species in clade 15 (including *R. sangzhiensis*) occur in the lowlands of Southwest China and adjacent northern Vietnam.

The DEC and DEC+J models both suggest an "Out of Asia" pattern involving two independent dispersals from East Asia into the New World (Fig. 4a), and a third one into Europe and Central Asia (Fig. 4b). This basic biogeographic pattern was established 48–25 Ma.

Under DEC, a range expansion approximately 48–43 Ma (Eocene) from East Asia into eastern North America (across northern North America) was followed by a vicariance event at 43 Ma. Subsequently, a second range expansion from East Asia to western North America (south along the Pacific coast of North America) occurred approximately 43–34 Ma (Eocene) followed by vicariance at 34 Ma, which restricted the *R. boylii* group (*Amerana*) to western North America. Under DEC+J, range evolution would be explained by jump dispersal, which is "instantaneous" speciation. The first such event (to eastern North America) occurred at 43 Ma, and the second (to western North America) at 34 Ma.

Are these models supported by geological and paleoecological information? During the Eocene (56–34 Ma), a continuous belt of boreotropical forest extended over the entire Northern Hemisphere from Asia through North America across Beringia (Wolfe 1975, 1987). This would have allowed considerable trans-Beringian exchange of terrestrial biota adapted to warm-temperate climates (Tiffney 1985a). Thus, during the early branching of *Rana*, it seems there was no obvious barrier to dispersal across Beringia. In the mid-Tertiary, beginning about 35 Ma, mixed deciduous hardwood and coniferous forests began to dominate in Beringia (Wolfe 1987), which perhaps facilitated the second dispersal of *Rana* (clade 13). The end of the Eocene event marked a dramatic climatic change (Sanmartín et al. 2001) from a "greenhouse" to an "icehouse" world. From 14–10 Ma to 3.5 Ma, cold taiga forest covered the Beringia bridge (Wolfe 1987), rendering additional dispersals of *Rana* unlikely. Asia and North America remained joined by Beringia until the opening of the Bering Strait at 5.5 or 5.3 Ma (Marincovich and Gladenkov 1999; Gladenkov et al. 2002).

The lack of a dispersal barrier suggests that range expansion to North America can be explained by DEC without including the J parameter. Under DEC+J, jump dispersal is typically associated with an inhospitable barrier such as ocean separating two continents or islands (Matzke 2013b).

The third major event, the occupation of Europe and Central Asia (Fig. 5b) from East Asia, took place from 29 to 25 Ma (under DEC; ambiguity in the reconstruction might push the 29 Ma limit back to 34 Ma). This event corresponds with the receding of the Turgai Sea at 30–29 Ma, which likely acted as a barrier for biotic exchanges between Europe and Asia from the Jurassic to the Eocene (Briggs 1995; Sanmartín et al. 2001). The ancestor of clade 17, which occupied Europe + Central Asia, experienced vicariance at 20 Ma. This isolated *R. asiatica* in Central Asia from its sister group, the European *R. temporaria* group. DEC+J depicts the two range shifts as a jump dispersal from East Asia to Europe at 25 Ma, followed by jump dispersal from Europe back to Central Asia at 20 Ma (Fig. 3). Progressive aridification of Central Asia beginning about 22 Ma (Guo et al. 2008) may have contributed to the present disjunction between the European *R. temporaria* group, *R. asiatica*, and clade 18 (the remaining East Asian species). Savage (1973) first proposed that this aridification event led to the range disjunction of the amphibian faunas of Europe and East Asia, and our analyses support this hypothesis for *Rana*. Other amphibian groups that may fit this pattern include *Bombina* (Zheng et al. 2009), *Hyla* (Li et al. 2015), and two clades within Salamandridae (Zhang et al. 2008).

Finally, expansion of *Rana* into South America occurred across the Isthmus of Panama. The three strictly South American species of *Rana* form a single clade that originated 16 Ma, and then diversified by 9 Ma (Fig. 3).

This finding supports dispersal across the Panamanian Isthmus in the middle Miocene, which is consistent with recent geological evidence that supports the formation of the Panamanian Isthmus at this time (Montes et al. 2015).

Although vicariance appears to have played a dominant role in speciation, strict geographic barriers do not appear to have been present in all speciation events. Heterogeneous landscapes, facilitated by differentiation in ecological dimensions, may have also driven speciation. The three New World areas (Fig. 2) are effectively ecological islands for speciation in *Rana*; almost no widespread species range across any two regions. The Mexican Plateau, as the transition zone between temperate and tropical regions, provides unique and restricted habitats that may drive ecological speciation. This might explain the numerous endemic species associated with this biodiversity hotspot (e.g., Mittermeier et al. 2005). Under DEC+J, dispersals from eastern NA to the Mexican Plateau and Neotropics appear to have occurred since the late Eocene, approximately 36 Ma. In the Neogene, we inferred frequent dispersals and speciation events (Fig. 3b). This jump-dispersal scenario for American *Rana* taxa should be further tested with other taxa, such as pitvipers and bunchgrass lizards (Castoe et al. 2009; Bryson et al. 2012).

Trans-Atlantic versus Trans-Beringian Dispersal

Our biogeographic analysis supports two independent dispersals of *Rana* from East Asia to North America via the Beringian land bridges (Fig. 2: H1b). In contrast, the hypothesis of a trans-Atlantic bridge connecting North America and Europe, as suggested by Case (1978) and illustrated in Figure 2 (H2), received little statistical support (Supplementary Table S9, available on Dryad). The trans-Atlantic dispersal route does not seem likely based on geological considerations. According to the ancestral range reconstructions for model H2 (Supplementary Fig. S6e, available on Dryad), one jump dispersal (DEC+J) or range expansion (DEC) from East Asia to Europe would have had to occur prior to the trans-Atlantic dispersal between Europe and eastern North America. The dispersal from East Asia to Europe would have had to occur by 48 Ma, but the Turgai Sea separated Asia from Europe at that time. Only after 30–29 Ma (Briggs 1995; Sanmartín et al. 2001) were extensive biotic exchanges between Europe and Asia possible. The lack of a sister-group relationship between the *Rana* of Europe and North America also argues strongly against the trans-Atlantic scenario.

The disjunct distributions of many taxa across the Holarctic region have attracted considerable attention of botanists and zoologists (e.g., Wen 1999; Sanmartín et al. 2001; Donoghue and Smith 2004). Most groups of temperate forest plants originated and diversified in eastern Asia, and then dispersed out of Asia across Beringia, mostly during the last 30 Ma (Donoghue and Smith 2004). In contrast, no general "Out of Asia" pattern has been reported for terrestrial animals. However, most terrestrial animal examples involve insects, birds, and mammals (Sanmartín et al. 2001). Do amphibians and reptiles show similar biogeographic patterns to plants, or to insects, birds, and mammals?

A considerable body of literature exists on the relationships of amphibians and reptiles that are endemic to at least two of the following major Holarctic regions: Europe, East Asia, western North America, and eastern North America. There have been 28 hypothesized dispersal events of amphibians and reptiles among these four regions (Table 1; Fig. 7). Amphibians involved in these dispersal events include groups of Cryptobranchidae, Salamandridae, Proteidae, Plethodontidae, Hylidae, and Ranidae (this study), and reptiles include Elapidae, Viperidae, Natricinae, Lampropeltini, Scincidae, Alligatoridae, Trionychidae, Emydidae, Geoemydidae, and Testudinidae (Table 1; Spinks et al. 2004; Min et al. 2005; Smith et al. 2005; Le et al. 2006, 2014; Macey et al. 2006; Burbrink and Lawson 2007; Roos et al. 2007; Vieites and Wake 2007; Le and McCord 2008; Pramuk et al. 2008; Wüster et al. 2008; Zhang et al. 2008, Zhang and Wake 2009; Hua et al. 2009; Kelly et al. 2009; Spinks and Shaffer 2009; Van Bocxlaer et al. 2010; Brandley et al. 2011; Garcia-Porta et al. 2012; Guo et al. 2012; Pyron et al. 2013; Pyron 2014; Li et al. 2015). Although Proteidae is also distributed in North America and Europe, the divergence between the relevant taxa is older than the breakup of Laurasia (108 Ma; Pyron 2014), and so Proteidae is not included in these comparisons. The remainder of the estimated dispersal times for the amphibians and reptiles ranged from the Early Eocene to the Middle Miocene (Table 1). The biogeographic origins of these clades largely fit the pattern seen among Holarctic plants (Donoghue and Smith 2004), with strong and repeated support for trans-Beringian over trans-Atlantic dispersal (Fig. 7). In contrast, support exists for just three trans-Atlantic dispersals (Salamandridae and Plethodontidae; Zhang et al. 2008; Zheng et al. 2009; and Emydidae; Spinks and Shaffer 2009).

Lineage Diversification in the Old versus New World

The lineages of Old and New World *Rana* have different trajectories of diversification (Figs. 5 and 6). Of the two clades that resulted from trans-Beringian dispersals, *Amerana* (clade 13, western North America), does not seem to have greatly influenced New World diversity. In contrast, clade 3, comprising the species of eastern North America, the Mexican Plateau, and the Neotropics rapidly radiated (Figs. 5b and 6b; 0.17 species/Ma), probably owing to the availability of diverse new ecological opportunities. BAMM analyses suggest a diversity-dependent process (Fig. 6b; Rabosky et al. 2007), resulting in saturation of ecological niche space and a decline in the speciation rate (Walker and Valentine 1984; Valentine 1985; Rabosky and Lovette 2008).

TABLE 1. Disjunct distributions of Eurasian and North American amphibians and reptiles

Taxa	Disjunction pattern number, direction of dispersal, and estimated divergence time (Ma, in parentheses)								Reference(s)
	A–E	A–C	A–D	C–D	C–E	D–E	A–NA	C–NA	
Cryptobranchidae	1, A to E (43)								Zhang and Wake (2009); Pyron (2014)
Ranidae (*Rana*)	2, A to E (43)	17, A to C (25)	13, A to D (34)						This study
Salamandridae (Modern Eurasia newts)		18, C to A (27)							Zhang et al. (2008); Pyron (2014)
Salamandridae (Primitive Eurasia newts)		19, C to A (27)							Zhang et al. (2008); Pyron (2014)
Salamandridae (*Taricha* and *Notophthalmus*)						27, ? (35)			Zhang et al. (2008); Pyron (2014)
Salamandridae (New World salamandrids)								24, C to NA (43.5)	Zhang et al. (2008); Pyron (2014)
Plethodontidae (*Hydromantes*)				25, D to C (33)					Pyron (2014); Vieites and Wake (2007)
Plethodontidae (*Karsenia*)							12, NA to A (51)		Pyron (2014); Min et al. (2005); Vieites and Wake (2007)
Plethodontidae (*Aneides*)						26, ? (40)			Pyron (2014); Vieites and Wake (2007)
Plethodontidae (*Plethodon*)						28, ? (50)			Pyron (2014); Vieites and Wake (2007)
Hylidae (*Hyla*)	7, E to A (16)	20, A to C (27)							Li et al. (2015); Pyron (2014)
Scincidae (*Plestiodon*)	3, A to E (24)								Brandley et al. (2011)
Scincidae (*Scincella*)	4, A to E (?)								Pyron et al. (2013)
Viperidae							11, A to NA (24)		Wüster et al. (2008)
Elapidae	6, A to E (25)								Kelly et al. (2009)
Colubrinae		22, A to C (26–25)					10, A to NA (26–25)		Burbrink and Lawson (2007)
Natricinae		21, A to C (27)					9, A to NA (27)		Guo et al. (2012)
Alligatoridae (*Alligator*)	8, E to A (53–47)								Wu et al. (2003); Roos et al. (2007)
Trionychidae (*Rafetus* and *Apalone*)	5, A to E (43)	15, A to C (21)							Le et al. (2014)
Emydidae (*Emys*)					23, E to C (17)				Spinks and Shaffer (2009)
Geoemydidae (*Mauremys*)		14, A to C (30–18)							Spinks et al. (2004); Le and McCord (2008)
Testudinidae (*Testudo*)		16, A to C (?)							Le et al. (2006)

Notes: Twenty-two clades with disjunct distributions are assigned to one of the eight two-area categories. Where the divisions of eastern and western North America are ambiguous, we combined them as North America (NA). "?" indicates that the time or place of origin is ambiguous. Numbers in parentheses represent the time of divergence (Ma). Numbered events refer to the disjunctions in Figure 7. Abbreviations: A, East Asia (mainland + islands); C, Europe; D, western North America; E, eastern North America. References refer to the phylogenetic studies from which data were obtained.

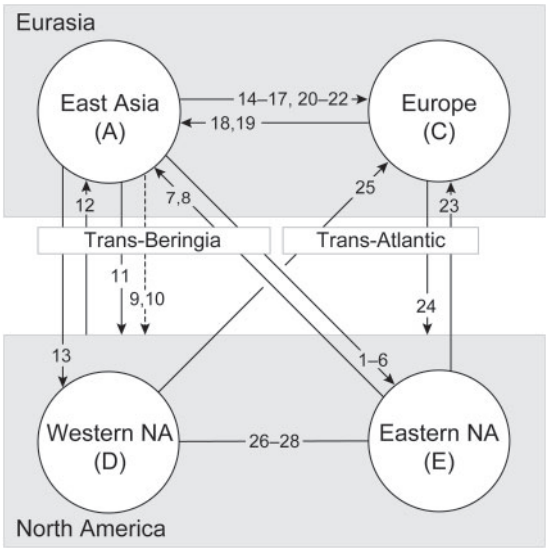

FIGURE 7. Inferred ancestral areas and directions of movement among the four major Holarctic areas for amphibians and reptiles. Letter designations for the major geographic areas are the same as in Figure 2 (A: East Asia; C: Europe; D: western North America; E: eastern North America). Arrows point from the inferred ancestral area to the newly colonized area. The line without arrowheads between eastern and western North America indicates three cases in which the direction of dispersal is ambiguous. The dotted line indicates two cases of possible (but somewhat ambiguous) trans-Beringian dispersal. Table 1 presents details for the 28 numbered inferred dispersal events.

A distinct increased rate of lineage accumulation occurred at around 14 Ma (clade 3; Fig. 5b), corresponding to dispersals among the Mexican Plateau, eastern North America, and Neotropics (Figs. 3 and 4c2), as well as *in situ* diversification of Mexican taxa. The rate increase generally corresponds to the Middle Miocene formation of the Trans-Mexican Volcanic Belt (Ferrari et al. 1999; Gómez-Tuena et al. 2007), which has likely contributed to the diversification of numerous taxa (e.g., Bryson et al. 2011, 2012).

In contrast, lineage accumulation of the Old World *Rana* (clades 1, 11, and 14) proceeded very slowly, then underwent a distinct net diversification rate-shift at around 29–18 Ma (about 1.4 species/Ma; Fig. 6c and Supplementary Figs. S7c and S8c, available on Dryad). Closing of the Turgai Strait after 29 Ma (Briggs 1995) permitted the dispersal of *Rana* into western Eurasia. Clade 17 further diversified in the Mediterranean region around 18 Ma, possibly in association with the onset of Asian monsoons at the Oligocene/Miocene boundary (Sun and Wang 2005).

Lineage accumulation of the East Asian clades 19–23 (Fig. 1) occurred over a short period of time (23–20 Ma) (Fig. 3) in association with island formation (Fig. 5b,d). From 23 to 15 Ma, rifting and tectonic deformation associated with block rotations and volcanism resulted in the substantial fragmentation of the East Asian margin and formation of islands as a continental sliver (Taira 2001; Itoh et al. 2006). Following the initial opening of the Sea of Japan in the Late Oligocene (Otofuji et al. 1985; Ingle 1992; Jolivet et al. 1994; Isozaki 1997; Taira 2001), the archipelagos of Japan rotated into their present configuration about 15 Ma (Taira 2001). The five clades (19–23; Fig. 1) along the Asian margin formed well before the origin of the present island system. Thus, our results support a role for Miocene tectonic events in the diversification of East Asian *Rana*.

Our analysis provides a framework for understanding and interpreting the biology of the well-studied frogs of the genus *Rana* throughout Eurasia and the Americas. Numerous studies of the biology of these frogs can be facilitated by a better understanding of their phylogeny and biogeography.

AUTHOR CONTRIBUTIONS

Conceived and designed the study: J.C., D.M.H., D.C.C., and Y.P.Z. Collected samples and sequence data: Z.Y.Y., W.W.Z., N.A.P., H.M.C., N.H.J.L., W.H.C., K.I., M.S.M., S.L.K., D.M.H., and J.C. Conducted and evaluated data analyses: Z.Y.Y., W.W.Z., X.C., N.J.M., D.C.C., D.M.H., and J.C. Discussed and drafted the manuscript: Z.Y.Y., W.W.Z., X.C., N.A.P., N.J.M., Y.P.Z., D.C.C., D.M.H., and J.C. All authors have read and approved the final version of the manuscript.

SUPPLEMENTARY MATERIAL

Data available from the Dryad Digital Repository: http://dx.doi.org/10.5061/dryad.ck1m7.

FUNDING

This work was supported by the Strategic Priority Research Program (B) Grant XDB13020200 of the Chinese Academy of Sciences (CAS) to J.C.; National Natural Science Foundation of China [31321002 to Y.P.Z., 31090250 to J.C., and 31401966 to W.W.Z.], the program of State Key Laboratory of Genetic Resources and Evolution, Kunming Institute of Zoology, CAS to N.A.P. [GREKF14-1], and a National Science Foundation Assembling the Tree of Life grant to DCC and DMH [AmphibiaTree; DEB 0334952]. J.C. was supported by the Youth Innovation Promotion Association CAS, and to study abroad in the University of Texas at Austin and the University of California at Berkeley by China scholarship council ([2014]3012) and Chinese Academy of Sciences ([2011]31). D.M.H. was supported for collaborative visits to the Kunming Institute of Zoology by an Einstein Professorship from the Chinese Academy of Sciences. N.A.P. was supported by the Russian Foundation of Basic Research [RFBR Taiwan 14-04-92000; RFBR 15-29-02771] and Russian Science Foundation [RSF 14-50-00029]. N.J.M. was supported by a NIMBioS fellowship under NSF Award [EFJ0832858], and ARC DECRA fellowship [DE150101773].

ACKNOWLEDGMENTS

We thank Jie-Qiong Jin for assisting with sample collection and laboratory work, Luke Mahler for the

use of his scripts, Jim McGuire for discussion regarding regional lineage accumulation, Mariana Vasconcellos for her help on biogeographic analyses, Shao-Yuan Wu and Bao-Lin Zhang for their help on species-tree analyses, Ted Papenfuss for discussions regarding transcontinental dispersals of amphibians and reptiles, Robert W. Murphy for suggestions on the manuscript, and Richard Glor and three anonymous reviewers for valuable suggestions during manuscript review. Amy Lathrop and Jingting Liu assisted in figure production.

REFERENCES

Alfaro M.E., Santini F., Brock C., Alamillo H., Dornburg A., Rabosky D.L., Carnevale G., Harmon L.J. 2009. Nine exceptional radiations plus high turnover explain species diversity in jawed vertebrates. Proc. Natl. Acad. Sci. USA. 106:13410–13414.

AmphibiaWeb. 2015. Information on amphibian biology and conservation. Berkeley (CA): University of California. Available from: URL http://amphibiaweb.org/ (Accessed July 2015).

Bossuyt F., Brown R.M., Hillis D.M., Cannatella D.C., Milinkovitch M.C. 2006. Phylogeny and biogeography of a cosmopolitan frog radiation: Late Cretaceous diversification resulted in continent-scale endemism in the family Ranidae. Syst. Biol. 55:579–594.

Boulenger G.A. 1920. A monograph of the American frogs of the genus *Rana*. Proc. Am. Acad. Arts Sci. 55:413–480.

Böhme M. 2001. The oldest representative of a brown frog (Ranidae) from the Early Miocene of Germany. Acta Paleontol. Polonica. 46:119–124.

Brandley M.C., Wang Y.Z., Guo X.G., de Oca A.N.M., Feria-Ortiz M., Hikida T., Ota H. 2011. Accommodating heterogeneous rates of evolution in molecular divergence dating methods: an example using intercontinental dispersal of *Plestiodon* (*Eumeces*) lizards. Syst. Biol. 60:3–15.

Briggs J.C. 1995. Global biogeography. Amsterdam: Elsevier Science.

Briggs R., King T.J. 1952. Transplantation of living nuclei from blastula cells into enucleated frogs' eggs. Proc. Natl. Acad. Sci. USA. 38:455–463.

Bryson R.W., Murphy R.W., Lathrop A., Lazcano-Villareal D. 2011. Evolutionary drivers of phylogeographical diversity in the highlands of Mexico: a case study of the *Crotalus triseriatus* species group of montane rattlesnakes. J. Biogeogr. 38:697–710.

Bryson R.W., García-Vázquez U.O., Riddle B.R. 2012. Relative roles of Neogene vicariance and Quaternary climate change on the historical diversification of bunchgrass lizards (*Sceloporus scalaris* group) in Mexico. Mol. Phylogenet. Evol. 62:447–457.

Burbrink F.T., Lawson R. 2007. How and when did Old World ratsnakes disperse into the New World? Mol. Phylogenet. Evol. 43:173–189.

Case S.M. 1978. Biochemical systematics of members of the genus *Rana* native to western North America. Syst. Zool. 27:299–311.

Castoe T.A., Daza J.M., Smith E.N., Sasa M.M., Kuch U., Campbell J.A., Chippindale P.T., Parkinson C.L. 2009. Comparative phylogeography of pitvipers suggests a consensus of ancient Middle American highland biogeography. J. Biogeogr. 36:88–103.

Che J., Pang J., Zhao E.M., Matsui M., Zhang Y.P. 2007a. Phylogenetic relationships of the Chinese brown frogs genus *Rana* inferred from partial mitochondrial 12S and 16S rRNA gene sequences. Zool. Sci. 24:71–80.

Che J., Pang J., Zhao H., Wu G., Zhao E.M., Zhang Y.P. 2007b. Phylogeny of Raninae Anura: Ranidae inferred from mitochondrial and nuclear sequences. Mol. Phylogenet. Evol. 43:1–13.

Derryberry E.P., Claramunt S., Derryberry G., Chesser R.T., Cracraft J., Aleixo A., Pérez-Emán J., Remsen J.V. Jr., Brumfield R.T. 2011. Lineage diversification and morphological evolution in a large-scale continental radiation: the neotropical ovenbirds and woodcreepers (Aves: Furnariidae). Evolution 65:2973–2986.

Donoghue M.J., Smith S.A. 2004. Patterns in the assembly of temperate forests around the Northern Hemisphere. Philos. Trans. R. Soc. Lond. B Biol. Sci. 359:1633–1644.

Drummond A.J., Ho S.Y.W., Phillips M.J., Rambaut A. 2006. Relaxed phylogenetics and dating with confidence. PLoS Biol. 4:e88.

Drummond A.J., Suchard M.A., Xie D., Rambaut A. 2012. Bayesian phylogenetics with BEAUti and the BEAST 1.7. Mol. Biol. Evol. 29:1969–1973.

Dubois A. 2006. Naming taxa from cladograms: a cautionary tale. Mol. Phylogenet. Evol. 42:317–330.

Dubois A. 1992. Notes sur la classification des Ranidae (Amphibiens Anoures). Bull. Soc. Linn. Lyon 61:305–352.

Duellman W.E., Trueb L. 1986. Biology of amphibians. Baltimore (MD): Johns Hopkins University Press.

Farris J.S., Kluge A.G., Mickevich M.F. 1980. Paraphyly of the *Rana boylii* group. Syst. Zool. 28:627–634.

Farris J.S., Kluge A.G., Mickevich M.F. 1983. Immunological distance and the phylogenetic relationships of the *Rana boylii* species group. Syst. Zool. 31:479–491.

Fei L., Hu S.Q., Ye C.Y., Huang Y.Z. 2012. Fauna Sinica, Amphibia Anura, Vol. 1. Beijing, China: Science Press.

Fei L., Ye C.Y., Huang Y.Z. 1990. Key to Chinese amphibians. Chongqing, China: Publishing House for Scientific and Technological Literature.

Ferrari L., Lopez-Martinez M., Aguirre-Diaz G., Carrasco-Nuñez G. 1999. Space-time patterns of Cenozoic arc volcanism in central Mexico: from the Sierra Madre Occidental to the Mexican Volcanic Belt. Geology 27:303–306.

Frost D.R. 2015. Amphibian species of the World: an online reference. Version 6.0. New York, USA: American Museum of Natural History. Available from: URL http://research.amnh.org/herpetology/amphibia/index.html (accessed July 2015).

Frost D.R., Grant T., Faivovich J., Bain R.H., Haas A., Haddad C.F.B., de Sá R.O., Channing A., Wilkinson M., Donnellan S.C., Raxworthy C.J., Campbell J.A., Blotto B.L., Moler P.E., Drewes R.C., Nussbaum R.A., Lynch J.D., Green D.M., Wheeler W.C. 2006. The amphibian tree of life. Bull. Am. Mus. Nat. Hist. 297:1–370.

Garcia-Porta J., Litvinchuk S.N., Crochet P.A., Romano A., Geniez P.H., Lo-Valvo M., Lymberakis P., Carranza S. 2012. Molecular phylogenetics and historical biogeography of the west-palearctic common toads (*Bufo bufo* species complex). Mol. Phylogenet. Evol. 63:113–130.

Gaston K.J. 2000. Global patterns in biodiversity. Nature 40:220–227.

Gladenkov Y.A., Oleinik A.E., Marincovich J.L., Barinov K.B. 2002. A refined age for the earliest opening of Bering Strait. Palaeogeogr. Palaeclimatol. Palaeoecol. 183:321–328.

Gómez-Tuena A., Langmuir C.H., Goldstein S.L., Straub S.M., Ortega-Gutierrez F. 2007. Geochemical evidence for slab melting in the Trans-Mexican Volcanic Belt. J. Petrol. 48:537–562.

Guo P., Liu Q., Xu Y., Jiang K., Hou M., Ding L., Pyron R.A., Burbrink F.T. 2012. Out of Asia: natricine snakes support the Cenozoic Beringian dispersal hypothesis. Mol. Phylogenet. Evol. 63:825–833.

Guo Z., Sun B., Zhang Z., Peng S., Xiao G., Ge J., Hao Q., Qiao Y., Liang M., Liu J. 2008. A major reorganization of Asian climate by the early Miocene. Clim. Past 4:153–174.

Harmon L.J., Weir J.T., Brock C.D., Glor R.E., Challenger W. 2008. GEIGER: investigating evolutionary radiations. Bioinformatics 24:129–131.

Hillis D.M. 1988. Systematics of the *Rana pipiens* complex: puzzle and paradigm. Ann. Rev. Ecol. Syst. 19:39–63.

Hillis D.M. 2007. Constraints in naming parts of the Tree of Life. Mol. Phylogenet. Evol. 42:331–338.

Hillis D.M., Davis S.K. 1986. Evolution of ribosomal DNA: fifty million years of recorded history in the frog genus *Rana*. Evolution 40:1275–1288.

Hillis D.M., de Sá R. 1988. Phylogeny and taxonomy of the *Rana palmipes* group (Salientia: Ranidae). Herpetol. Monogr. 2:1–26.

Hillis D.M., Frost J.S., Webb R.G. 1984. A new species of frog of the *Rana tarahumarae* group from southwestern Mexico. Copeia 1984:398–403.

Hillis D.M., Frost J.S., Wright D.A. 1983. Phylogeny and biogeography of the *Rana pipiens* complex: a biochemical evaluation. Syst. Zool. 32:132–143.

Hillis D.M., Wilcox T.P. 2005. Phylogeny of the New World true frogs (*Rana*). Mol. Phylogenet. Evol. 34:299–314.

Holman J.A. 1965. Early Miocene anurans from Florida. J. Florida Acad. Sci. 28:68–82.

Holman J.A. 1968. Additional Miocene anurans from Florida. J. Florida Acad. Sci. 30:121–140.
Hua X., Fu C., Li J.T., de Oca A.N.M., Wiens J.J. 2009. A revised phylogeny of Holarctic treefrogs (genus *Hyla*) based on nuclear and mitochondrial DNA sequences. Herpetologica 65:246–259.
Ingle C.J. 1992. Subsidence of the Japan Sea: stratigraphic evidence from ODP sites and onshore sections, Proc. Ocean Drill. Program Sci. Results 127:1197–1218.
Isozaki Y. 1997. Contrasting two types of orogen in Permo-Triassic Japan: accretionary versus collisional. Isl. Arc. 6:2–24.
Itoh Y., Uno K., Arato H. 2006. Seismic evidence of divergent rifting and subsequent deformation in the southern Japan Sea, and a Cenozoic tectonic synthesis of the eastern Eurasian margin. J. Asian Earth Sci. 27:933–942.
Jiang J.K., Fei L., Ye C.Y., Zeng X.M., Xie F., Chen Y.Y., Zheng M.W. 1997. Studies on the taxonomics of species of *Pseudorana* and discussions on the phylogenetic relationships with its related genera. Cultum Herpetol. Sin. 6:67–74.
Jolivet L.K., Tamaki K., Fournier M. 1994. Japan Sea, opening history and mechanism: a synthesis. J. Geophys. Res. 99:22237–22259.
Kelly C.M.R., Barker N.P., Villet M.H., Broadley D.G. 2009. Phylogeny, biogeography and classification of the snake superfamily Elapoidea: a rapid radiation in the late Eocene. Cladistics 25:38–63.
Lanfear R., Calcott B., Ho S.Y.W., Guindon S. 2012. Partition finder: combined selection of partitioning schemes and substitution models for phylogenetic analyses. Mol. Biol. Evol. 29:1695–1701.
Le M., Duong H.T., Dinh L.D., Nguyen T.Q., Pritchard P.C.H., McCormack T. 2014. A phylogeny of softshell turtles (Testudines: Trionychidae) with reference to the taxonomic status of the critically endangered, giant softshell turtle, *Rafetus swinhoei*. Org. Divers. Evol. 14:279–293.
Le M., McCord W.P. 2008. Phylogenetic relationships and biogeographical history of the genus *Rhinoclemmys* Fitzinger, 1835 and the monophyly of the turtle family Geoemydidae (Testudines: Testudinoidea). Zool. J. Linn. Soc. 153:751–767.
Le M., Raxworthy C.J., McCord W.P., Mertz L. 2006. A molecular phylogeny of tortoises (Testudines: Testudinidae) based on mitochondrial and nuclear genes. Mol. Phylogenet. Evol. 40:517–531.
Li J.T., Wang J.S., Nian H.H., Litvinchuk S.N., Wang J., Li Y., Rao D.Q., Klaus S. 2015. Amphibians crossing the Bering Land Bridge: evidence from holarctic treefrogs (*Hyla*, Hylidae, Anura). Mol. Phylogenet. Evol. 87:80–90.
Liu C.C., Hu S.Q. 1961. Tailless amphibians of China. Beijing: Science Press.
Liu L., Yu L., Edwards S.V. 2010. A maximum pseudo-likelihood approach for estimating species trees under the coalescent model. BMC Evol. Biol. 10:302.
Macey J.R., Schulte J.A., Strasburg J.L., Brisson J.A., Larson A., Ananjeva N.B., Wang Y., Parham J.F., Papenfuss T.J. 2006. Assembly of the eastern North American herpetofauna: new evidence from lizards and frogs. Biol. Lett. 2:388–392.
Mahler D.L., Revell L.J., Glor R.E., Losos J.B. 2010. Ecological opportunity and the rate of morphological evolution in the diversification of Greater Antillean anoles. Evolution 64:2731–2745.
Marincovich J.L., Gladenkov A.Y. 1999. Evidence for an early opening of the Bering Strait. Nature 397:149–151.
Matsui M. 2011. On the brown frogs from the Ryukyu Archipelago, Japan, with descriptions of two new species Amphibia, Anura. Curr. Herpetol. 302:111–128.
Matzke N.J. 2013a. BioGeoBEARS: biogeography with Bayesian and likelihood evolutionary analysis in R scripts. Available from: http://cran.r-project.org/web/packages/BioGeoBEARS/ (accessed 5 March 2014).
Matzke N.J. 2013b. Probabilistic historical biogeography: new models for founder-event speciation, imperfect detection, and fossils allow improved accuracy and model testing. Front. Biogeogr. 5:242–248.
Matzke N.J. 2014. Model selection in historical biogeography reveals that founder-event speciation is a crucial process in island clades. Syst. Biol. 63:951–970.
McGuire J.A., Witt C.C., Remsen J.V. Jr., Corl A., Rabosky D.L., Altshuler D.L., Dudley R. 2014. Molecular phylogenetics and the diversification of hummingbirds. Curr. Biol. 24:910–916.
McPeek M.A., Brown J.M. 2007. Clade age and not diversification rate explains species richness among animal taxa. Am. Nat. 169:E97–E106.
Min M.S., Yang S.Y., Bonett R.M., Vieites D.R., Brandon R.A., Wake D.B. 2005. Discovery of the first Asian plethodontid salamander. Nature 435:87–90.
Mirarab S., Reaz R., Bayzid M.S., Zimmermann T., Swenson M.S., Warnow T. 2014. ASTRAL: genome-scale coalescent-based species tree estimation. Bioinformatics 30:541–548.
Mittelbach G.G., Schemske D.W., Cornell H.V., Allen A.P., Brown J.M., Bush M.B., Harrison S.P., Hurlbert A.H., Knowlton N., Lessios H.A., McCain C.M., McCune A.R., McDade L.A., McPeek M.A., Near T.J., Price T.D., Ricklefs R.E., Roy K., Sax D.F., Schluter D.H., Sobel J.M., Turelli M. 2007. Evolution and the latitudinal diversity gradient: speciation, extinction and biogeography. Ecol. Lett. 10:315–331.
Mittermeier R.A., Gil P.R., Hoffman M., Pilgrim J., Brooks T., Mittermeier C.G., Lamoreux J., da Fonseca G.A.B. 2005. Hotspots revisited: Earth's biologically richest and most endangered terrestrial ecoregions. Washington (DC): Conservation International.
Montes C., Cardona A., Jaramillo C., Pardo A., Silva J.C., Valencia V., Ayala C., Pérez-Angel L.C., Rodriguez-Parra L.A., Ramirez V., Niño H. 2015. Middle Miocene closure of the Central American Seaway. Science 348:226–229.
Moyle R.G., Andersen M.J., Oliveros C.H., Steinheimer F.D., Reddy S. 2012. Phylogeny and biogeography of the Core Babblers (Aves: Timaliidae). Syst. Biol. 61:631–651.
Near T.J., Bolnick D.I., Wainwright P.C. 2005. Fossil calibrations and molecular time divergence estimates in centrarchid fishes (Teleostei: Centrarchidae). Evolution 59:1768–1782.
Nylander J., Wilgenbusch J., Warren D., Swofford D. 2008. AWTY (are we there yet?): a system for graphical exploration of MCMC convergence in Bayesian phylogenetics. Bioinformatics 24:581.
Otofuji Y., Matsuda T., Nohda S. 1985. Paleomagnetic evidences for the Miocene counterclockwise rotation of northeast Japan-Rifting process of the Japan arc. Earth Planet. Sci. Lett. 75:265–277.
Paradis E., Claude J., Strimmer K. 2004. APE: analyses of phylogenetics and evolution in R language. Bioinformatics 20:289–290.
Parmley D., Hunter K.B., Holman J.A. 2010. Fossil frogs from the Clarendonian (Late Miocene) of Oklahoma, U.S.A. J. Vertebr. Paleontol. 30:1879–1883.
Plummer M., Best N., Cowles K., Vines K. 2006. CODA: convergence diagnosis and output analysis for MCMC. R News. 6:7–11.
Post T.J., Uzzell T. 1981. The relationships of *Rana sylvatica* and the monophyly of the *Rana boylii* group. Syst. Zool. 30:170–180.
Pyron R.A. 2014. Biogeographic analyses reveals ancient continental vicariance and recent oceanic dispersal in Amphibia. Syst. Biol. 63:779–797.
Pyron R.A., Burbrink F.T., Wiens J.J. 2013. A phylogeny and revised classification of Squamata, including 4161 species of lizards and snakes. BMC Evol. Biol. 13:93.
Pramuk J.B., Robertson T., Sites J.W., Noonan B.P. 2008. Around the world in 10 million years: biogeography of the nearly cosmopolitan true toads (Anura: Bufonidae). Glob. Ecol. Biogeogr. 17:72–83.
Qian H., Ricklefs R.E. 2000. Large-scale processes and the Asian bias in species diversity of temperate plants. Nature 407:180–182.
Rabosky D.L. 2009. Ecological limits and diversification rate: alternative paradigms to explain the variation in species richness among clades and regions. Ecol. Lett. 128:735–743.
Rabosky D.L. 2014. Automatic detection of key innovations, rate shifts, and diversity-dependence on phylogenetic trees. PLoS One 92:e89543.
Rabosky D.L., Donnellan S.C., Talaba A.L., Lovette I.J. 2007. Exceptional among-lineage variation in diversification rates during the radiation of Australia's most diverse vertebrate clade. Proc. R. Soc. B 274:2915–2923.
Rabosky D.L, Lovette I.J. 2008. Density-dependent diversification in North American wood warblers. Proc. R. Soc. B 275:2363–2371.
Rabosky D.L., Santini F., Eastman J., Smith S.A., Sidlauskas B., Chang J., Alfaro M.E. 2013. Rates of speciation and morphological evolution are correlated across the largest vertebrate radiation. Nat. Commun. 4:1958.

Rambaut A., Drummond A. 2007. Tracer v1.4. Available from: URL http://beast.bio.ed.ac.uk/Tracer.
R Core Development Team. 2014. R: a language and environment for statistical computing. Vienna, Austria: R Foundation for Statistical Computing.
Ree R.H., Smith S.A. 2008. Maximum likelihood inference of geographic range evolution by dispersal, local extinction, and cladogenesis. Syst. Biol. 57:4–14.
Ricklefs R.E. 2004. A comprehensive framework for global patterns in biodiversity. Ecol. Lett. 7:1–15.
Ronquist F., Huelsenbeck J.P. 2003. MrBayes 3: Bayesian phylogenetic inference under mixed models. Bioinformatics 19:1572.
Roos J., Agarwal R.K., Janke A. 2007. Extended mitogenomic phylogenetic analyses yield new insight into crocodilian evolution and their survival of the Cretaceous–Tertiary boundary. Mol. Phylogenet. Evol. 45:663–673.
Savage J.M. 1973. The geographic distribution of frogs: patterns and predictions. In: Vial J.L., editor, Evolutionary biology of the anurans. Columbia: University of Missouri Press. p. 351–445.
Savage R.M. 1962. The ecology and life history of the common frog (*Rana temporaria temporaria*). New York: Hafner Publication Company.
Sambrook J., Fritsch E., Maniatis T. 1989. Molecular cloning: a laboratory manual. 2nd ed. New York: Cold Spring Harbor Laboratory Press.
Sanmartín I., Enghoff H., Ronquist F. 2001. Patterns of animal dispersal, vicariance and diversification in the Holarctic. Biol. J. Linn. Soc. 73:345–390.
Schluter D. 2001. Ecology of adaptive radiation. Trends Ecol. Evol. 16:372–380.
Shaw T., Ruan Z., Glenn T., Liu L. 2013. STRAW: species tree analysis web server. Nucleic Acids Res. 41:W230–W241.
Smith S.A., Stephens P.R., Wiens J.J. 2005. Replicate patterns of species richness, historical biogeography, and phylogeny in Holarctic treefrogs. Evolution 59:2433–2450.
Spinks P.Q., Thomson R.C., Lovely G.A., Shaffer H.B. 2009. Assessing what is needed to resolve a molecular phylogeny: simulations and empirical data from emydid turtles. BMC Evol. Biol. 9:56.
Spinks P.Q., Shaffer H.B. 2009. Conflicting mitochondrial and nuclear phylogenies for the widely disjunct *Emys* (Testudines: Emydidae) species complex, and what they tell us about biogeography and hybridization. Syst. Biol. 58:1–20.
Spinks P.Q., Shaffer H.B., Iverson J.B., McCord W.P. 2004. Phylogenetic hypotheses for the turtle family Geoemydidae. Mol. Phylogenet. Evol. 32:164–182.
Sun X.J., Wang P.X. 2005. How old is the Asian monsoon system?—Palaeobotanical records from China. Palaeogeogr. Palaeoclimatol. Palaeoecol. 222:181–222.
Stamatakis A. 2006. RAxML-VI-HPC: maximum likelihood-based phylogenetic analyses with thousands of taxa and mixed models. Bioinformatics 22:2688–2690.
Stuart B.L. 2008. The phylogenetic problem of *Huia* (Amphibia: Ranidae). Mol. Phylogenet. Evol. 46:49–60.
Swofford D.L. 2003. PAUP*: phylogenetic analysis using parsimony * and other methods. Version 40b10. Sunderland (MA): Sinauer Associates.
Taira A. 2001. Tectonic evolution of the Japanese island arc system. Annu. Rev. Earth Planet. Sci. 29:109–134.
Tamura K., Peterson D., Peterson N., Stecher G., Nei M., Kumar S. 2011. MEGA5: Molecular evolutionary genetics analysis using maximum likelihood, evolutionary distance, and maximum parsimony methods. Mol. Phylogenet. Evol. 28:2731–2739.
Tanaka-Ueno T., Matsui M., Chen S.L., Takennaka O., Ota H. 1998. Phylogenetic relationship of brown frogs from Taiwan and Japan assessed by mitochondrial cytb gene sequence *Rana*: Ranidae. Zool. Sci. 15:283–288.
Tanaka T., Matsui M., Takenaka O. 1996. Phylogenetic relationships of Japanese brown frogs Ranidae: *Rana* assessed by mitochondrial cytochrome b gene sequences. Biochem. Syst. Ecol. 24:299–307.
Thompson J.D., Gibson T.J., Plewniak F., Jeanmougin F., Higgins D.G. 1997. The CLUSTAL X windows interface: flexible strategies for multiple sequence alignment aided by quality analysis tools. Nucleic Acids Res. 25:4876–4882.
Tiffney B.H. 1985a. Perspectives on the origin of the floristic similarity between eastern Asia and eastern North America. J. Arnold Arbor. 66:73–94.
Tiffney B.H. 1985b. The Eocene North Atlantic land bridge: its importance in Tertiary and modern phytogeography of the Northern Hemisphere. J. Arnold Arbor. 66:243–273.
Valentine J.W. 1985. Biotic diversity and clade diversity. In: Valentine J.W., editor. Phanerozoic diversity patterns. Princeton (NJ): Princeton University Press. p. 419–424.
Van Bocxlaer I., Loader S.P., Roelants K., Biju S.D., Menegon M., Bossuyt F. 2010. Gradual adaptation toward a range-expansion phenotype initiated the global radiation of toads. Science 327:679–682.
Veith M., Kosuch J., Vences M. 2003. Climatic oscillations triggered post-Messinian speciation of Western Palearctic brown frogs Amphibia, Ranidae. Mol. Phylogenet. Evol. 26:310–327.
Vieites D.R., Wake D.B. 2007. Rapid diversification and dispersal during periods of global warming by plethodontid salamanders. Proc. Natl. Acad. Sci. USA. 104:19903–19907.
Voorhies M.R., Holman J.A., Xiang-Xu X. 1987. The Hottell Ranch rhino quarries (basal Ogallala: medial Barstovian), Banner County, Nebraska. Part I: Geological setting, faunal lists, lower vertebrates.Contrib. Geol. Univ. Wyoming. 25: 55–69.
Walker T.D., Valentine J.W. 1984. Equilibrium models of evolutionary species diversity and the number of empty niches. Am. Nat. 124:887–899.
Wen J. 1999. Evolution of eastern Asian and eastern North American disjunct distributions in flowering plants. Ann. Rev. Ecol. Syst. 30:421–455.
Wiens J.J., Donoghue M.J. 2004. Historical biogeography, ecology and species richness. Trends Ecol. Evol. 19:639–644.
Wiens J.J., Sukumaran J., Pyron R.A., Brown R.M. 2009. Evolutionary and biogeographic origins of high tropical diversity in Old World frogs (Ranidae). Evolution 63:1217–1231.
Wolfe J.A. 1975. Some aspects of plant geography in the Northern Hemisphere during the late Cretaceous and Tertiary. Ann. Missouri Bot. Gard. 62:264–279.
Wolfe J.A. 1987. Late Cretaceous–Cenozoic history of (Ursidae) inferred from complete sequences of deciduousness and the terminal Cretaceous event. Paleobiology 16:215–226.
Wu X., Wang Y., Zhou K., Zhu W., Nie J., Wang C. 2003. Complete mitochondrial DNA sequence of Chinese alligator, *Alligator sinensis*, and phylogeny of crocodiles. Chin. Sci. Bull. 48: 2050–2054.
Wüster W., Peppin L., Pook C.E., Walker D.E. 2008. A nesting of vipers: phylogeny and historical biogeography of the Viperidae (Squamata: Serpentes). Mol. Phylogenet. Evol. 49:445–459.
Xia X., Xie Z. 2001. DAMBE: software package for data analysis in molecular biology and evolution. J. Hered. 92:371–373.
Ye C.Y., Fei L., Hu S.Q. 1993. Rare and economic amphibians of China. Chengdu, China: Sichuan Publishing House of Science and Technology.
Zhang P., Papenfuss T.J., Wake M.H., Qu L., Wake D.B. 2008. Phylogeny and biogeography of the family Salamandridae (Amphibia: Caudata) inferred from complete mitochondrial genomes. Mol. Phylogenet. Evol. 49:586–597.
Zhang P., Wake D.B. 2009. Higher-level salamander relationships and divergence dates inferred from complete mitochondrial genomes. Mol. Phylogenet. Evol. 53:492–508.
Zheng Y.C., Fu J.Z., Li S.Q. 2009. Toward understanding the distribution of Laurasian frogs: A test of Savage's biogeographical hypothesis using the genus *Bombina*. Mol. Phylogenet. Evol. 52:70–83.
Zweifel R.G. 1955. The ecology and systematics of the *Rana boylii* species group. Univ. Cal. Publ. Zool. 54:207–292.